



Precision Optics Manufacturing and Control for Next-Generation Large Telescopes

Logan R. Graves¹ · Greg A. Smith¹ · Dániel Apai^{2,3} · Dae Wook Kim^{1,2}

Received: 2 December 2018 / Revised: 4 February 2019 / Accepted: 7 February 2019

© International Society for Nanomanufacturing and Tianjin University and Springer Nature Singapore Pte Ltd. 2019

Abstract

Next-generation astronomical telescopes will offer unprecedented observational and scientific capabilities to look deeper into the heavens, observe closer in time to the epoch of the Big Bang, and resolve finer details of phenomena throughout the universe. The science case for this next generation of observatories is clear, with science goals such as the discovery and exploration of extrasolar planets, exploration of dark matter and dark energy, the formation and evolution of planets, stars, galaxies, and detailed studies of the Sun. Enabling breakthrough astronomical goals requires novel and cutting-edge design choices at all stages of telescope manufacturing. In this paper, we discuss the integrated design and manufacturing of the next-generation large telescopes, from the optical design to enclosures required for optimal performance.

Keywords Metrology · Fabrication · Design · Telescope · Optics · Precision

1 Introduction

Astronomers studying new phenomena and testing increasingly detailed models of the universe require ever more powerful instruments to complete their goals and collect photons which have traversed immense distances and time, sometimes originating at the very beginning of the universe. From Edwin Hubble's measurements of the Doppler-shifts of galaxies, through studies of high redshift supernova explosions that revealed the acceleration of the universe to the latest studies of exoplanet atmospheric composition, astronomical knowledge has most often been limited by the number of photons that could be efficiently collected. Phenomena such as first light observations, exoplanet studies, dark matter, galaxy and planet formation, and other topics require ever more advanced scientific instruments. For a detailed analysis of these science goals, the reader is encouraged to explore resources such as the *GMT Science Book* [1] or *An*

Expanding View of the Universe—Science with the European Extremely Large Telescope [2]. To provide these scientific capacities and to advance instrumentation capabilities, the next generation of telescopes (NGT) must provide higher spatial resolutions, larger light-collecting areas, and more sensitive instrumentation. These telescopes are each unique in their designs, from primary mirror and instrumentation design choices to the observatory sites and dome designs. However, they all share the goal of improving our understanding of the universe by providing advanced instruments for astronomical observations.

One family of fascinating telescope design concepts currently being implemented is that of extremely large telescopes. Since the 1.5 cm telescope made by Galileo in 1609, there has always been a push for larger light-collecting areas [3]. In the 19th century, there were rapid improvements in telescopes, beginning with the 60-inch (1.5 m) telescope in 1908, which was eclipsed by the Hooker telescope with a 2.5-m aperture in 1917. It was not until 1949 that the Hale Telescope took the record for the largest telescope aperture at 5.1-m, held until the BTA-6 telescope was introduced in 1975 with a 6-m aperture. Since then, the Keck 1 with a 10-m aperture in 1993, the LBT with two 8.4-m primary mirrors in 2005, and the Gran Telescopio Canarias with a 10.4-m aperture in 2009 have defined the largest telescopes in the world. Figure 1 demonstrates this evolution of telescope mirror diameters over time.

✉ Dae Wook Kim
letter2dwk@hotmail.com

¹ College of Optical Sciences, University of Arizona, 1630 E. University Blvd., Tucson, AZ 85721, USA

² Steward Observatory, University of Arizona, 933 N. Cherry Ave., Tucson, AZ 85718, USA

³ Lunar and Planetary Laboratory, University of Arizona, 1629 E. Univ. Blvd., Tucson, AZ 85718, USA

Fig. 1 Primary mirror diameter has grown more than two orders of magnitude in the last three centuries and shows no sign of slowing down. The next generation of extremely large telescopes will use segmented reflectors to increase mirror size by a factor of 3 or more within the next decade

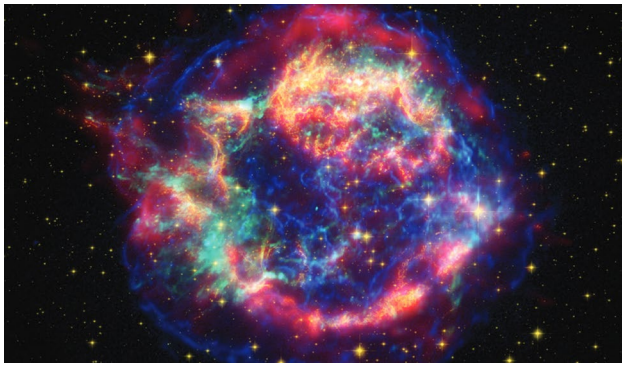
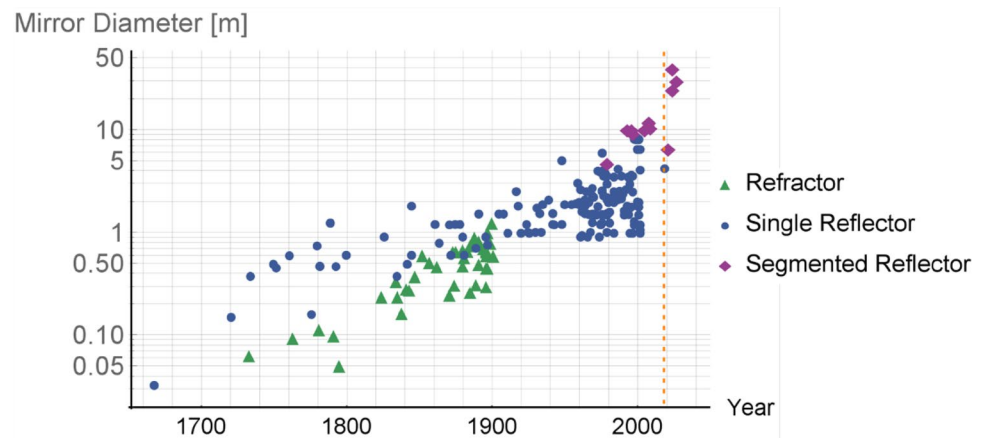


Fig. 2 One primary focus of the next generation of telescopes will be improved observational abilities of extremely faint phenomenon, such as the studies of supernova remnants, in conjunction with other telescopes. This is illustrated by the false color image of the remnants of supernova Cassiopeia A. This image uses data from the Spitzer Space Telescope (red), optical data from the Hubble Space Telescope (orange), and X-ray data from the Chandra X-ray Observatory (green) to display detailed structure. We can expect improved data from the next generation of telescopes to be used to provide a deeper look into such phenomenon [8]

Spanning more than two orders of magnitude in the last three centuries, the need for larger apertures shows no signs of slowing down. The extremely large telescopes, whose primary apertures will range from 20 to 40 m, are scheduled for first light as soon as 2024. Currently, three such telescopes are being fabricated and will be operational in the near future: the Giant Magellan Telescope (GMT) [4], the European Extremely Large Telescope (E-ELT) [5], and the Thirty Meter Telescope (TMT) [6, 7]. Despite sharing the designation of being extremely large telescopes, each system has unique design choices, from mirror substrate materials to adaptive optics approaches. However, all three extremely large telescopes share the feature of having enormous primary mirror collecting areas. This will enable not only greater light-collecting capability, allowing astronomers to observe fainter

phenomenon in the universe, such as that shown in Fig. 2, but will also provide greater resolving power (spatial resolution) and higher image quality. A combination of spatial resolution, high image contrast, and sensitivity will be key, for example, to the imaging search for Earth-sized extrasolar planets in the solar neighborhood.

The current consensus is that a segmented primary mirror design is the best approach to create the light-collecting areas beyond that of 8.5-m diameter mirrors. The GMT consists of seven such circular aperture segments, each of which is an 8.4-m diameter monolithic borosilicate honeycomb structure [4]. The E-ELT and TMT primary mirrors are constructed of significantly more numerous, but smaller and thinner segments [5, 6]. Different designs have led to different fabrication approaches. GMT requires precise manufacturing over large areas. Each segment will be fabricated to have a root-mean-square (RMS) surface figure error in the 20 nm range after mirror bending modes are corrected. Six of the segments are off-axis parabolic structures and the central segment is an on-axis mirror with a central aperture. In contrast, the E-ELT and TMT have relatively more rapid fabrication processes per mirror segment. To maximize effective optical aperture size covered by mirrors in the final assembly, the segments will be hexagonal in shape. This requires unique fabrication methodologies, such as using Computer Numeric Control (CNC) machining, to achieve the desired mirror shape. For example, the E-ELT will utilize 798 hexagonal segments that are each roughly 1.45 m point to point and have unique freeform shapes [9]. While the fabrication processes for these extremely large primary mirrors is automated as much as practical, maintaining surface accuracy is a non-trivial process.

These extremely large ground-based telescopes will not operate in isolation. Their scientific observations will guide other ground-based observatories as well as observational programs on space-based telescopes [10]. The James Webb Space Telescope (JWST), scheduled for launch in 2021, uses a novel design in which 18 hexagonal,

gold-coated beryllium segments make up the primary mirror. Surface RMS error is ~ 23 nm over a total diameter of 6.5 m, providing a significantly larger collecting area than the Hubble Space Telescope (HST) with its 2.4-m diameter design [11]. Unlike the HST, which observes at wavelengths ranging from near-ultraviolet to the near-infrared (0.2–2.3 μm), the JWST will be observing significantly deeper in the infrared wavelength range (0.6–27 μm). The JWST will be deployed to the L_2 Lagrange point between the Earth and Sun, and a large foldable sun shield made of aluminum and silicon-coated Kapton will improve telescope performance by keeping the telescope itself extremely cold throughout its mission.

Complementing these telescopes designed to probe deeper into the universe is the Large Synoptic Survey Telescope (LSST), whose goal is to provide time-domain observations by surveying extremely large swaths of the night sky. The system utilizes a single 8.4-m primary, similar to the GMT segments, and will have a final f -number of $f/1.23$ with a field of view (FOV) of 9.6 square degrees [12]. The LSST also utilizes a novel CCD camera system to accommodate the large FOV and sensitivity requirements, which is coupled with large bandpass filters having high optical requirements [13]. Part of the unique optical design of the LSST is a combined primary/tertiary mirror, requiring meticulous fabrication and metrology [14], as well as a custom telescope mount assembly [15]. Figure 3 demonstrates a portion of the process for fabricating both mirrors from a single glass blank.

The LSST is designed primarily for visible wavelengths, imaging from 320 to 1050 nm, and will spend approximately 90% of its observing time devoted to a

deep-wide-fast survey mode. The data obtained is expected to include a catalog of 20 billion galaxies and a similar number of stars. This library will improve our scientific understanding of the universe and will provide valuable survey data for the global array of astronomical telescopes to examine in depth.

Another key area of observation which will soon benefit from next-generation telescopes is solar observations. The Daniel K. Inouye Solar Telescope (DKIST) is a 4.2-m aperture solar telescope which is expected to begin operations in 2019. The primary mirror is a 4.2-m off-axis parabolic surface fabricated from a monolithic piece of Zerodur glass with a super-smooth surface finish [16]. The system will provide spectro-polarimetry from the visible to near-infrared bands as well as advanced imaging tools to investigate solar flares, make coronagraphic observations of the prominence-cavity structure, and measure coronal magnetic fields among other studies.

Enabling these ambitious scientific programs requires advances in other supporting technologies as well. For the ground-based extremely large telescopes, advanced adaptive and active optical control are essential to achieve the system requirements. The GMT will utilize a segmented secondary mirror which provides active and adaptive control via driving actuators mounted onto a Zerodur support structure [17]. These systems, combined with active control of the primary segments, provide multiple different seeing modes for the telescope. On the other hand, the E-ELT system does not introduce a deformable mirror until after the first three mirrors in the optical path [9]. The fourth and fifth mirrors in the system provide adaptive optics control of the post-focus beam. All these design choices have tradeoffs and highlight

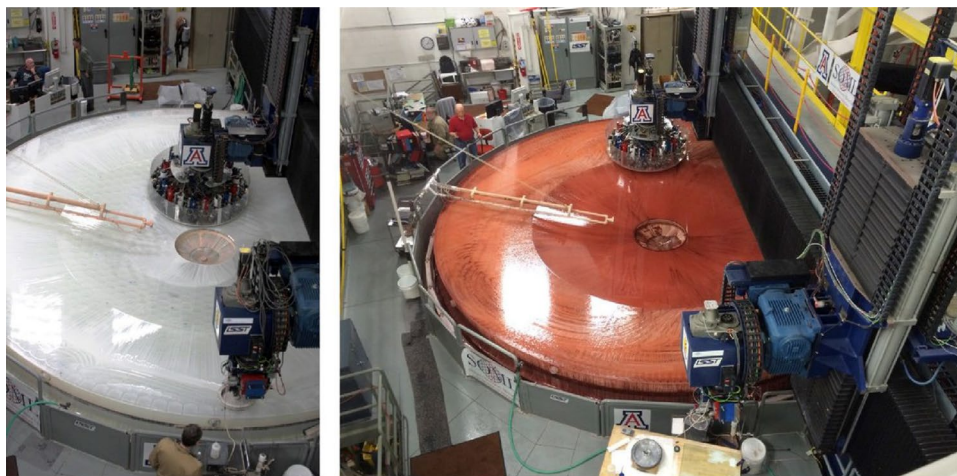


Fig. 3 The LSST primary/tertiary mirror is a coupled optic with an outer diameter of 8.4 m. This coupled design allows for a compact optical layout and powers the extremely wide FOV of the LSST. A 1.2-m stressed lap was used on the tertiary mirror while a 25-cm orbital lap was used on the primary mirror simultaneously using zir-

conium oxide as a polishing compound (left). A stressed lap polish on the tertiary mirror was also performed using iron oxide (right), and better highlights the disparity in curvature of the two mirror portions [14]

the diverse range of optical design choices that can be made within the scope of extremely large optics.

While adaptive optics control is essential for correction of atmospheric-induced aberrations, active mirror control and phasing are also required for all of the NGT systems. One key component that is used for both adaptive and active optics are wavefront sensors. Each telescope system has a unique wavefront-sensing approach, different in design and location within the system. The TMT, for example, plans to utilize a series of sodium laser guide stars to help direct its adaptive and active optic control [18]. Additionally, unique tip/tilt on-instrument wavefront sensors will be used for dedicated tip/tilt/focus sensing in the near-infrared. The JWST presents another interesting demand in which the primary mirrors and secondary mirror will all have to be phased and aligned in space after deployment [19]. To achieve the required active mirror control and phasing a complex iterative approach has been developed, which will combine wavefront sensing with other approaches, as shown in Fig. 4.

Once the telescope systems are aligned, active and adaptive control has begun, and phasing of the segments is completed (when applicable), the NGTs will begin recording data. However, the demands on the systems do not diminish at this stage. For the ground-based systems, wind, earthquakes, gravity, and thermal effects can compromise the precise alignment required from the systems. These factors are coupled with the requirement that the telescopes track their targets at high speeds and with great precision.

The extremely large telescope structures require novel designs to meet the size, accuracy, and speed requirements. While traditionally telescope domes have vertically sliding shutters, the sheer size of the required apertures for the extremely large telescopes made this approach undesirable. Thus, the GMT, E-ELT, and TMT all have different methods of achieving the required viewing aperture for the telescopes [20]. One commonality is that a horizontally opening aperture is frequently used. The DKIST design is an exception because it has tighter requirements on fast and accurate tracking of the sun with the aperture. This demand drove the enclosure design to make use of a novel crawler track which, when coupled with the overall enclosure design, allows for fast azimuthal and horizon tracking of the sun to high accuracy [21]. Other concerns such as minimizing stray light and wind control are major drivers in the design choices of the enclosures. Minimizing turbulence/convection in the airflow throughout the dome and providing stable/uniform temperature control of the telescope are also critical to reduce dome-seeing. Mounting stability and stiffness must be considered as well for such enormous and heavy structures and components, particularly when mirror positioning accuracy is of prime importance.

With telescopes going on-line as soon as 2019, the next generation of telescopes is finally upon us, ushering in a new era of global astronomical science. At all levels, these systems require novel technologies to enable new

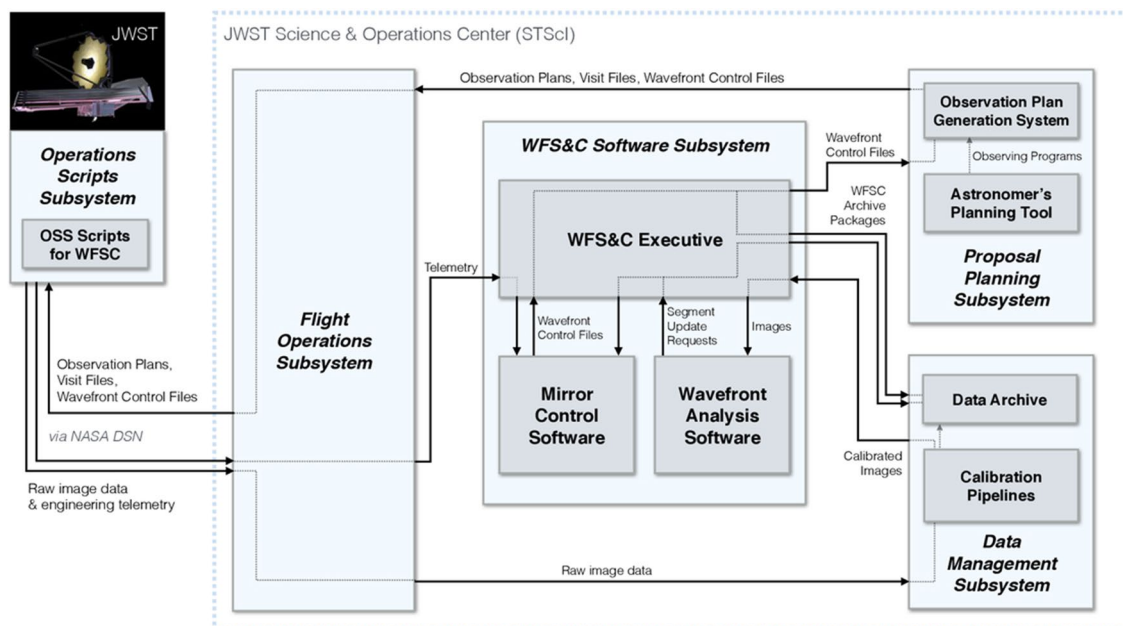


Fig. 4 The JWST must achieve and maintain proper mirror phasing and positioning once it reaches the proper orbit in space. Because further adjustments become prohibitively challenges once launched, the

JWST will have a robust system for this alignment. The telescope utilizes a complex system, whose flow chart is shown, to provide active mirror positioning, mirror phasing and wavefront analysis [19]

breakthrough science. This paper seeks to summarize the methods utilized to create these powerful and timeless scientific instruments, which remain in use often for over a century.

2 Telescope Optical System Design

A key aspect enabling the science in the NGTs are the optics in the system, from the primary and secondary mirrors to overall optical design. Primary mirrors for the next generation of telescopes will use freeform shapes to achieve improved imaging quality. Freeform optics, optical surfaces which deviate from a standard spherical shape and typically are non-axisymmetric, have become increasingly integral in modern optical systems [22]. Further, a wider range of materials, from the standard borosilicate glass to the more exotic Zerodur and beryllium are being used to fabricate telescope optics. The primary mirror overall shapes additionally extend from standard circular apertures to hexagonal apertures. Thus, there is a wealth of new techniques and science being employed in the design of the NGT primary mirrors.

The extremely large telescopes are one area pushing the primary mirror optical design. Unfortunately, there is no practical way to handle (during a manufacturing process), test (requiring an enormous test tower), assemble (with an optical accuracy), and ship (to the final observatory site) a monolithic over 20-m in diameter precision mirror. To create such large primary mirrors, the fabrication consensus has been to fabricate multiple mirror segments which will be combined to create the overall primary mirror for these systems. To satisfy this approach, the GMT makes use of 8.4-m diameter segments, while the E-ELT and TMT utilize many smaller hexagonal segmented mirrors approximately 1.5-m in size. Each approach has unique fabrication and metrology requirements which impact other aspects of the design.

The GMT will provide observations across an extremely large spectrum, from 320 nm to 25 μm , and utilizes a fast-aplanatic Gregorian optical design with a final $f/8.2$ focus [17]. Figure 5 demonstrates the proposed GMT observatory. By using only seven segments for the primary mirror, phasing involves few parameters and the primary surface area (24.5 m diameter) is maximized. The segments are made of E6 low-expansion glass generated in a light-weighted honeycomb design. The telescope will provide a 20 arcmin FOV with a wide field of view corrector. The structure allows for 11 instruments to be simultaneously mounted with rapid optical path selection capability. The adaptive secondary mirror (ASM) is composed of seven 1.05-m segments which have deformable surfaces. Additionally, there exists a fast steering mirror

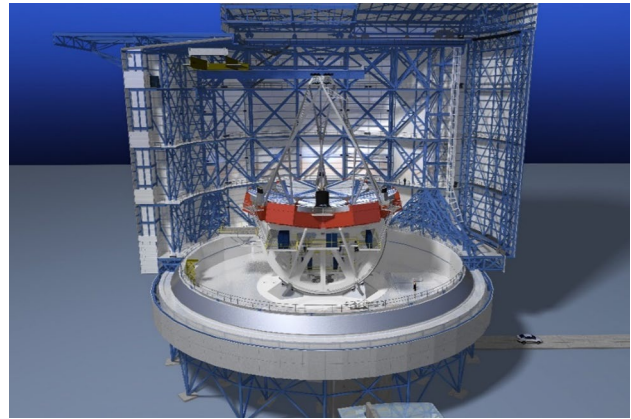


Fig. 5 The GMT telescope will be a relatively compact extremely large telescope. The optical design is a fast-aplanatic Gregorian design. The primary mirror is composed of seven 8.4-m diameter segments, for a total clear aperture diameter of 24.5 m. The secondary mirror is constructed from seven complimentary segments and will provide active and adaptive control. The final focus is located just below the primary mirror where instruments will be located for various observational studies. Image Credit: Giant Magellan Telescope GMTO Corporation

(FSM) assembly, composed of seven optically identical segments, which can be switched out for the ASM [17]. Of the primary mirror segments, six are highly aspheric, with up to 14 mm of aspheric departure. One beneficial aspect of both the ASM and FSM secondary assemblies is their ability to correct minor positioning errors of the primary segments, which greatly relaxes the opto-mechanical constraints on the structure. Finally, one of the more distinctive characteristics of the GMT system is its use of a direct focus, with the instrument platform located directly below the primary mirror. This departs from the increasingly common Nasmyth platform design choice and allows instruments to record light after only two reflections, from the primary and the secondary mirrors, increasing system efficiency and compactness.

The E-ELT, on the other hand, makes use of a series of segmented hexagonal mirrors to create a primary mirror with an overall diameter of 39 m. For the E-ELT, which is a three-mirror anastigmat design used on axis, the primary mirror will be constructed from 798 segments of special low-expansion Zerodur glass, which measure roughly 1.45 m from point to point and are 50 mm thick. Figure 6 shows the conceptual diagram of the final E-ELT telescope design. The use of smaller segments allows for more rapid fabrication, which is essential as the project schedule calls for extremely rapid production and installation of the segments [23]. The secondary mirror is a convex asphere measuring 4.1 m in diameter and will be located 30 m above the primary mirror. The tertiary mirror is a concave mild asphere which will be located near the vertex of the primary mirror and



Fig. 6 The E-ELT telescope, the largest of the extremely large NGTs, is a three-mirror anastigmat on-axis design. Nearly 800 individual hexagonal segments will be used to construct the primary mirror, which is 39 m in diameter. The light travels to a suspended convex secondary mirror 30 m above the primary and from there to a concave tertiary mild aspheric mirror. Flat adaptive mirrors guide the light to instruments, located on two Nasmyth structures. Image Credit: ESO

will measure 3.9 m in diameter [9]. The emerging beam is approximately $f/18$ at this point, and here the design departs significantly from the previously mentioned GMT in that two additional flat mirrors are used to guide the light to the Nasmyth focus. These flat mirrors—which constitute the fourth and fifth mirrors in the system—are a 2.5-m flat deformable mirror and a 3-m \times 2.5-m flat mirror, respectively. These mirrors will not only guide the beam but also provide atmospheric aberration correction.

The TMT telescope similarly will make use of 492 hexagonal segments that are 1.44 m point to point, 45 mm thick, and made from a special low-expansion Clearceram glass in order to create a primary mirror with a 30-m overall diameter [24]. The hexagonal design allows for tight packing of the segments and low weight, at the cost of a greater challenge of aligning and phasing so many mirrors. The TMT system will, for example, have over 10,000 degrees of freedom in the final system, all of which must be operating in precise coordination to achieve the required positioning and alignment of the system [25]. The telescope optical design is that of a Ritchey–Chrétien with an $f/1$ primary and an $f/15$ overall focus ratio [26]. Figure 7 highlights a cross section of the final system. The TMT has been designed with lessons learned from the Keck Observatory, and thus certain design and fabrication choices have been made to streamline

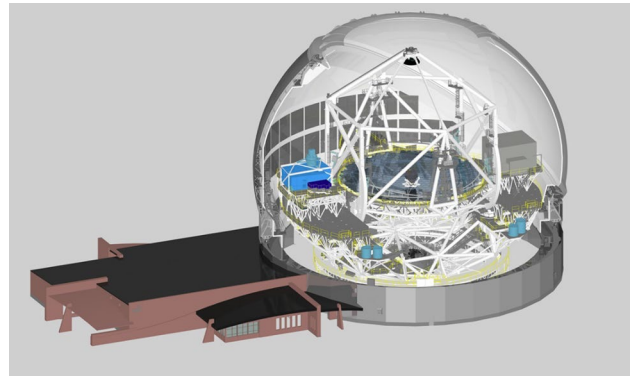


Fig. 7 The TMT telescope uses a Ritchey–Chrétien optical design which was guided by lessons learned from the Keck Observatory. Like the E-ELT, the primary mirror is composed of hundreds of hexagonal mirror segments. The secondary mirror is a hyperboloid which provides a final $f/15$ focus ratio. A tertiary flat mirror steers light to the Nasmyth structure, where instruments are located. Image Credit: TMT International Observatory

and improve the overall structure. The secondary mirror is a 3.6-m diameter hyperboloid which provides the final $f/15$ focus ratio, and a tertiary flat steering mirror will guide the light to a Nasmyth structure. The system is an optical-infrared telescope and the mirror coating will be a protected silver coating, which will provide high reflectivity and low emissivity in the planned imaging bands.

The JWST will make use of 18 hexagonal segments to construct its 6.5-m diameter primary mirror. However, the science requirements for JWST are significantly different from those of the ground-based telescopes discussed, and thus some unique design choices were made. The primary mirror segments are crafted from O30 Beryllium. To minimize the mass of the mirrors, they went through a final shaping process whereby much of the back side was removed, leaving a “rib” structure that keeps the segment shape steady. The light-weight segments thus have 92% of the original mass removed [27]. The mirrors were then polished and had a gold coating applied with a thin glass (SiO_2) protective overcoat to provide high reflectivity in the 0.6–28.5 μm infrared bands the telescope is designed for. The overall optical design is that of a three-mirror anastigmat (TMA). The light will be sent from the primary mirror to the secondary and from there to a protected tertiary mirror and finally to a fine steering mirror (FSM). The tertiary mirror is located behind the Cassegrain focus, while the FSM is located at the pupil image. The optical layout is shown in Fig. 8 and surrounded by a large solar shield to minimize thermal disruption.

Of course, not all the NGTs require a segmented primary mirror. The DKIST will make use of a single 4.2-m diameter off-axis parabolic primary mirror [16]. The mirror is a monolithic piece of Zerodur glass, which is essential to

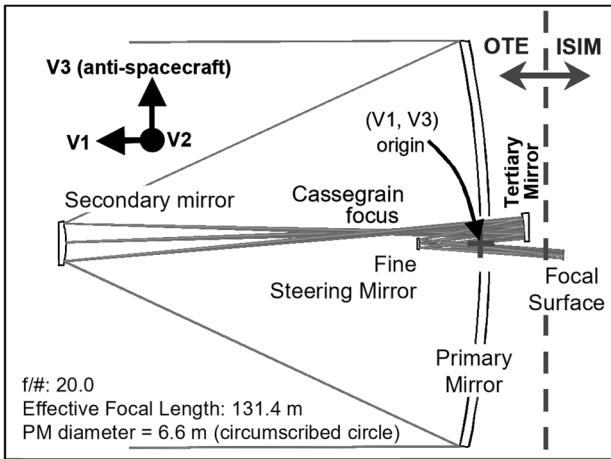
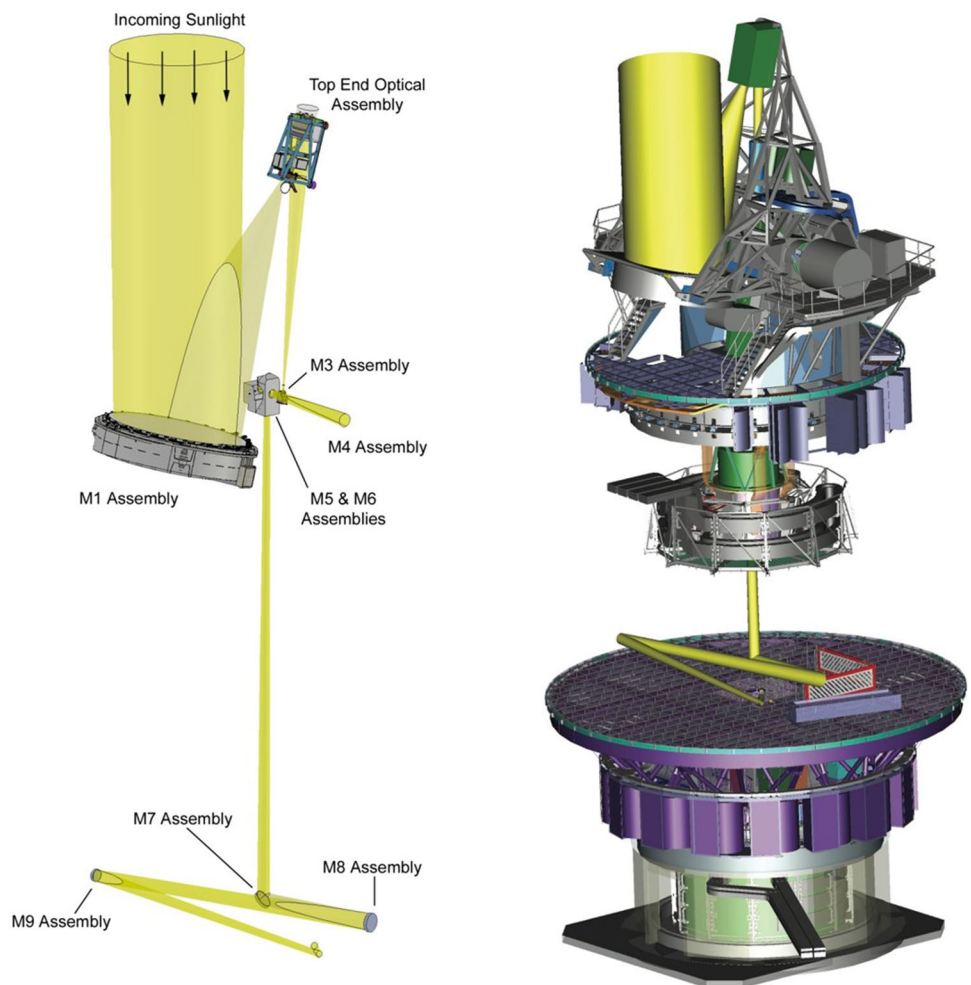


Fig. 8 The JWST will be the preeminent infrared space telescope when launched. Due to the constraints of launching a telescope, the design was guided strongly by minimizing weight and size. The system makes use of a three-mirror anastigmat design, allowing for minimal structure which still provides excellent optical performance. The telescope itself will unfold once it is deployed in space [27]

control thermal expansion during direct imaging of the Sun. Light is guided to a 70-cm-diameter secondary mirror which provides Gregorian focus with a 5 arcmin telescope FOV and a spectral range from 0.3 to 28 μm . Due to the intense thermal loads, the system will be exposed to the primary mirror must be actively cooled and must control the scattered light to less than 25×10^{-6} that of the solar disk irradiance at $R/R_{\text{sun}} = 1.1$ and $\lambda = 1 \mu\text{m}$ [28]. Because the goal of the DKIST is to provide premier observing capabilities of the Sun, a suite of tools will be located at the Gregorian focus which can obscure parts of the field to support specific observing goals. After the secondary mirror, the beam will be guided to further scientific instruments by eight additional mirrors, $M3$ – $M10$, where $M10$ is a deformable mirror. (Note: $M\#$ stands for the mirror number.) The DKIST full optical path is shown in Fig. 9.

Amid such diverse and unique optical design choices, one key commonality exists: freeform optics, which enable more compact optical system designs and highly tailored aberration control for specific science or optical applications. Whether segmented or monolithic, ground or space-based, circular or hexagonal, freeform optics are key enablers in

Fig. 9 The DKIST system will provide unprecedented observations of the Sun. The direct exposure to the Sun required for this mission calls for a novel design choice in the primary mirror to minimize thermal effect. The system uses a single monolithic Zerodur off-axis parabolic (OAP) primary mirror, which allows for the remaining optics to be in the optical path without obscuring the incoming beam. After the primary mirror, there are nine further mirrors which provide further beam focusing and steering to the science instruments [16]



the next generation of telescopes. This is a feature we can expect to see more of as today's fabrication and metrology teams have demonstrated their ability to create such optics to extreme precision.

3 Precision Manufacturing and Control Technology

3.1 Optical Fabrication Technologies

The design choices and theoretical performance of NGTs would amount to little without the capability to accurately fabricate the optics in the systems. The magnitude and complexity of surface shapes make for highly challenging fabrication processes. This challenge is compounded by the fact that the mirrors are made of different materials, over the course of a decade in some cases, and—after bending modes are applied—can only have a root-mean-square deviation from the ideal surface of tens of nanometers. However, not only have fabricators been able to deliver optics that meet all requirements, but they are now moving into higher efficiency and more streamlined methods which should allow for faster and more reliable production of advanced large optics. We explore some of the techniques being used to create the mirrors in these telescopes, from the materials to create the monolithic optics to the polishing and grinding tools used to generate the final surface figure. Today, multiple technologies are essential in freeform optical fabrication, including CNC machining and diamond turning and standard grinding and polishing as well as subaperture corrections via Magneto-Rheological Fluid (MRF) methods or other techniques [29–31].

It should be noted generally that several methods are used to generate the base surface of freeform optics. The optic shape can be achieved through CNC diamond turning, grinding of blanks, or even molded optics [32]. Diamond-turned optics can generate freeform shapes typically out of metal substrates with a multi-axis stage. The current limit on the precision that can be achieved with this technique is roughly 5 nm RMS, which, when followed by a smoothing run, can produce excellent freeform optical surfaces [33]. There are a range of other cutting methods which exist to shape precision surfaces. These techniques are essential in optical fabrication, allowing for nano- to micro level surface shaping [34].

One interesting technique which is sometimes applied for subaperture surface corrections is the MRF approach. This technique utilizes a magnetic fluid which can be precisely guided to polish a surface to a high-quality finish. It is extremely effective in the fabrication of freeform surfaces up to and larger than diameters of 300 mm, reliably achieving

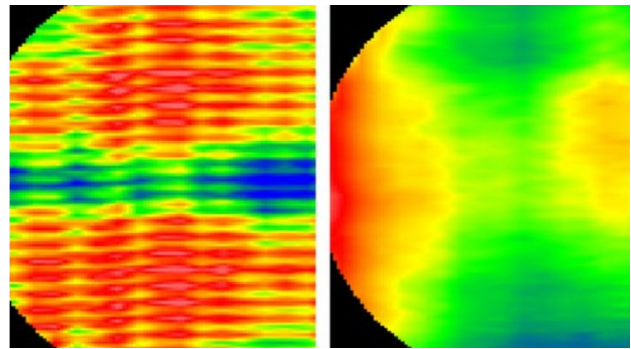


Fig. 10 Diamond turning involves using a diamond-tipped tool in combination with a CNC machine to achieve precise freeform fabrication over a variety of materials. After a first run, the process can leave mid-spatial frequencies on the optic surface (left). Thus a polishing run is required to smooth the mid-spatial frequencies out of the surface for the final optic (right) [29]

surface finishes on the order of 150 nm PV (Peak-to-Valley) and 20 nm RMS [35]. As shown in Fig. 10, by polishing the surface, residual mid-spatial frequencies generated during subaperture correction techniques can be effectively removed to produce a smooth optical surface.

In the case of the GMT primary mirrors, a large rotating furnace is used to generate the glass primary blanks. To achieve high stiffness and low weight, the mirrors make use of a honeycomb back design. Coarse shaping occurs with diamond wheel cutting followed by loose abrasive grinding to remove tooling marks. Final shaping and polishing use traditional polishing compounds and computer-controlled polishing [36–38] shown in Fig. 11.

In this method, a tool pad is set in an orbiting motion with a spatially-dependent dwell time to control glass removal rate. Recent innovations in polishing include an actuated tool pad that is able to dynamically change shape for more precise glass removal, as well as a rigid conformal tool which uses a non-Newtonian visco-elastic fluid as the tool pad. Figure 11 demonstrates the rigid conformal tool being used for polishing of a GMT segment, and the estimated and measured removal maps as well as the designed dwell time for optimal surface figuring.

In the case of the E-ELT and TMT, where hundreds of segments must be produced, the demand for an efficient and rapid fabrication process becomes even more important [40, 41]. For the E-ELT the process starts with cast circular mirror blanks which are ground and rough polished and then cut to their hexagonal shape using a CNC machine. A unique grolishing process then fits in between the grinding and polishing stages to remove mid-spatial frequency surface errors [42, 43]. Next, the segments are attached to their mounting fixtures and undergo a version of the bonnet polishing method with a rotating, precessing compliant spherical tool [23]. The tool rasters across the surface, and by adjusting

Fig. 11 A visco-elastic non-Newtonian fluid is used in the rigid conformal tool during GMT primary mirror segment polishing (a). The surface removal after polishing (b) closely matches the predicted removal (c), with a difference of only 97 nm RMS (d). The tool is guided by a dwell time map (e), generated by software which predicts material removal via parametric modeling [39]

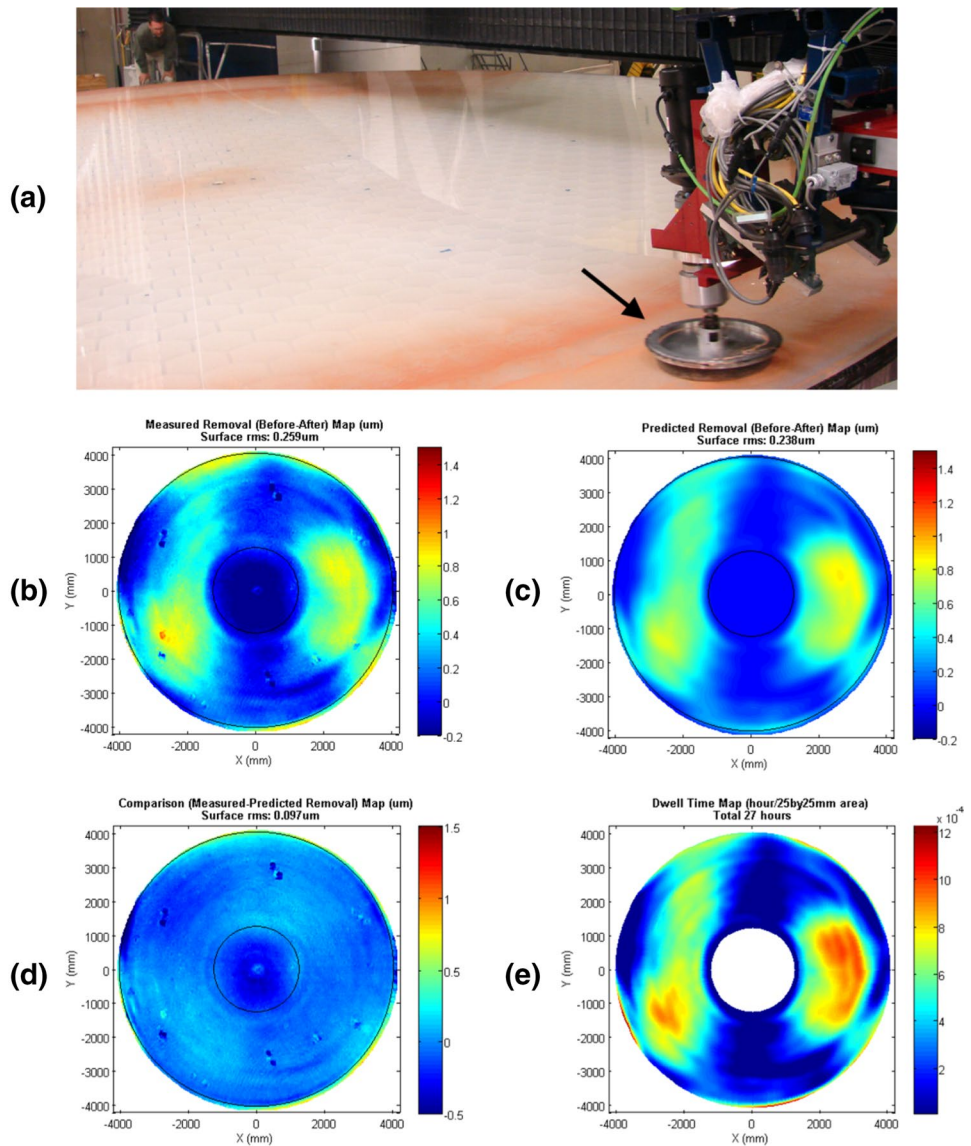
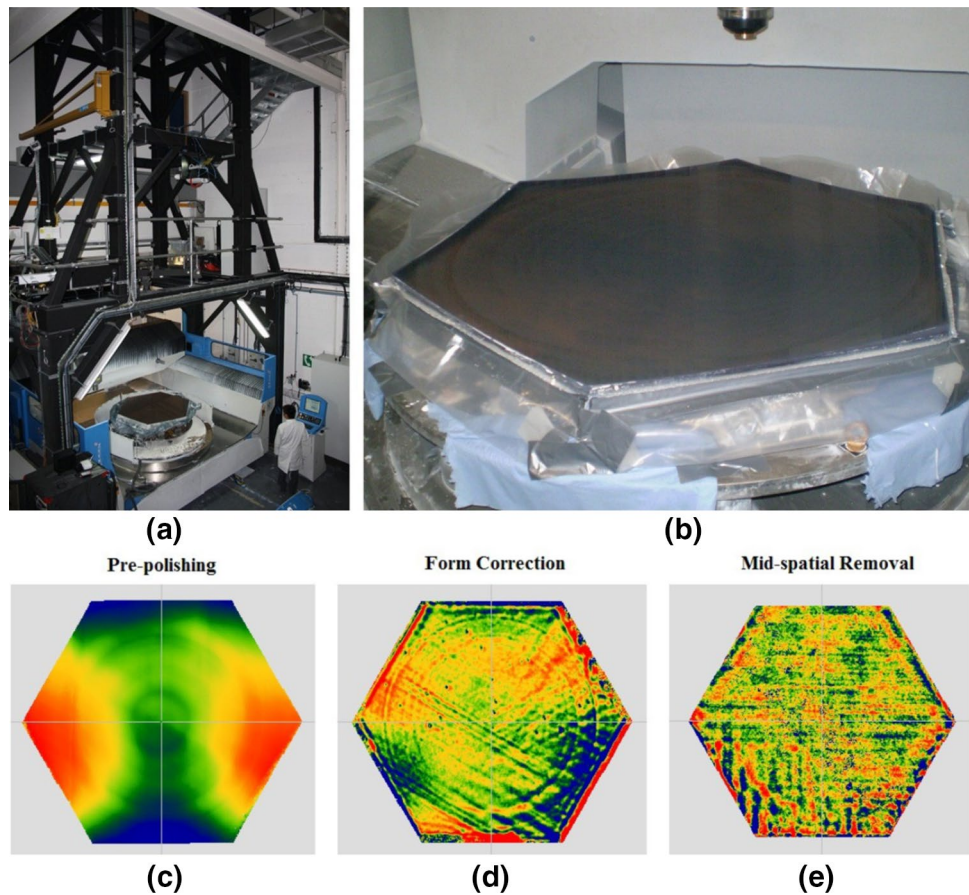


Fig. 12 The E-ELT primary mirror uses a multi-step process to generate the final mirror segments. Initially, a circular mirror blank is fabricated and sent for further processing (left). The circular mirror segments undergo grinding, and rough polishing. The mirror support

is then prepared for bonding and the segments are cut into their final hexagonal shape (right). The support and segment are assembled, and final polishing runs then occur. Image Credit: ESO/SCHOTT

Fig. 13 During fabrication of the E-ELT primary mirror segments a combined in situ metrology process was performed to streamline the fabrication. The mirror segment is mounted on a polishing machine which is located under a metrology test tower (a). The surface is then polished to achieve the desired surface figure (b). At the pre-polishing stage the optical surface is dominated by low spatial frequencies errors, such as astigmatism (c). After form correction (d) the mid-spatial frequencies are removed using a unique grolishing technique (e), which fits between the polishing and grinding phases [43]



the pressing strength, the glass removal rate is adjusted. Figure 12 demonstrates the flow of the mirror fabrication process from casting to mounted optic.

Complimenting this process is a full aperture test tower which the machine sits under, allowing for in situ testing between fabrication runs. The configuration of this test process, as well as the surface figure progression, is shown in Fig. 13.

It should be noted that careful calibration of all tooling previously mentioned must be performed for accurate fabrication. Laser trackers, reference balls, self-centering probes, and advanced methods including a multilateration approach for geometric verification of a machine tool are essential for calibration of machine geometry prior to and during fabrication [44].

The JWST had to take a significantly different approach when fabricating the primary mirror segments due to the material used. The mirror blanks were generated using an optical grade beryllium powder, which was loaded into a hexagonal enclosure and underwent a hot isostatic press process which converted the material into a solid. The solid mass was then cut into two equal blanks and light-weighted to reduce the 250-kg mass of a single blank down to 21 kg



Fig. 14 After precision fabrication of the JWST mirror segments, they require a special coating. Due to the target infrared imaging band, the mirror segments utilize a high uniformity gold coating, which is achieved via vapor deposition. This provides high reflectivity in the imaging bands targeted. Additionally, a protective overcoat layer is applied to help shield the optical surface from damage once deployed [45]

by machining out much of the back structure of the blank to leave a fine ‘rib’ structure for support. The blanks were then ground and polished and transported to various other test facilities between initial and final polishing. For the coating, a vapor deposition process was utilized which created a high-quality, high uniformity gold coating with a protective overlayer [45]. Figure 14 shows a completed segment after coating.

3.2 Advanced Metrology Solutions

It is essential to utilize advanced metrology methods to guide and verify the optical fabrication process. The challenge this presents has grown significantly as more extreme freeform designs and larger optics are being utilized. Broadly, the metrology techniques used can be broken down into two major categories; contact and non-contact metrology. Both approaches are essential to fabricate the described optics, and interesting advancements have been made across the board [46].

The metrology methods used to guide and verify the fabrication of the optics in the next generation of telescopes must meet the precision and accuracy demands as well as the efficiency requirements for the optics. For example, the E-ELT telescope primary will require a total of 960 primary mirror (M1) segments, which includes extra mirrors for the manufacturing yield provision, to be produced over a period of 84 months [47]. Each of the E-ELT M1 segments is unique in shape and must have a final surface figure error less than 25 nm across the clear aperture. The metrology must be able to (a) meet the tight accuracy requirements in a repeatable way for the freeform segments, and (b) must not slow down the fabrication cycle significantly. This requires efficiency to be a strong consideration in the employed metrology approaches which will be employed at various fabrication sites, while also maintaining nanometer level form accuracy [48, 49]. For example, the grinding phase of fabrication can rapidly approach the desired surface figure, but metrology becomes extremely challenging as the surface is not specularly reflective in the visible band. Thus, traditional high-precision optical metrology methods, such as visible interferometry, cannot be applied. It is in this region where advancements in metrology have led to greatly reduced fabrication times by improving the accuracy of rough surface metrology, allowing for more rapid convergence of surface shape.

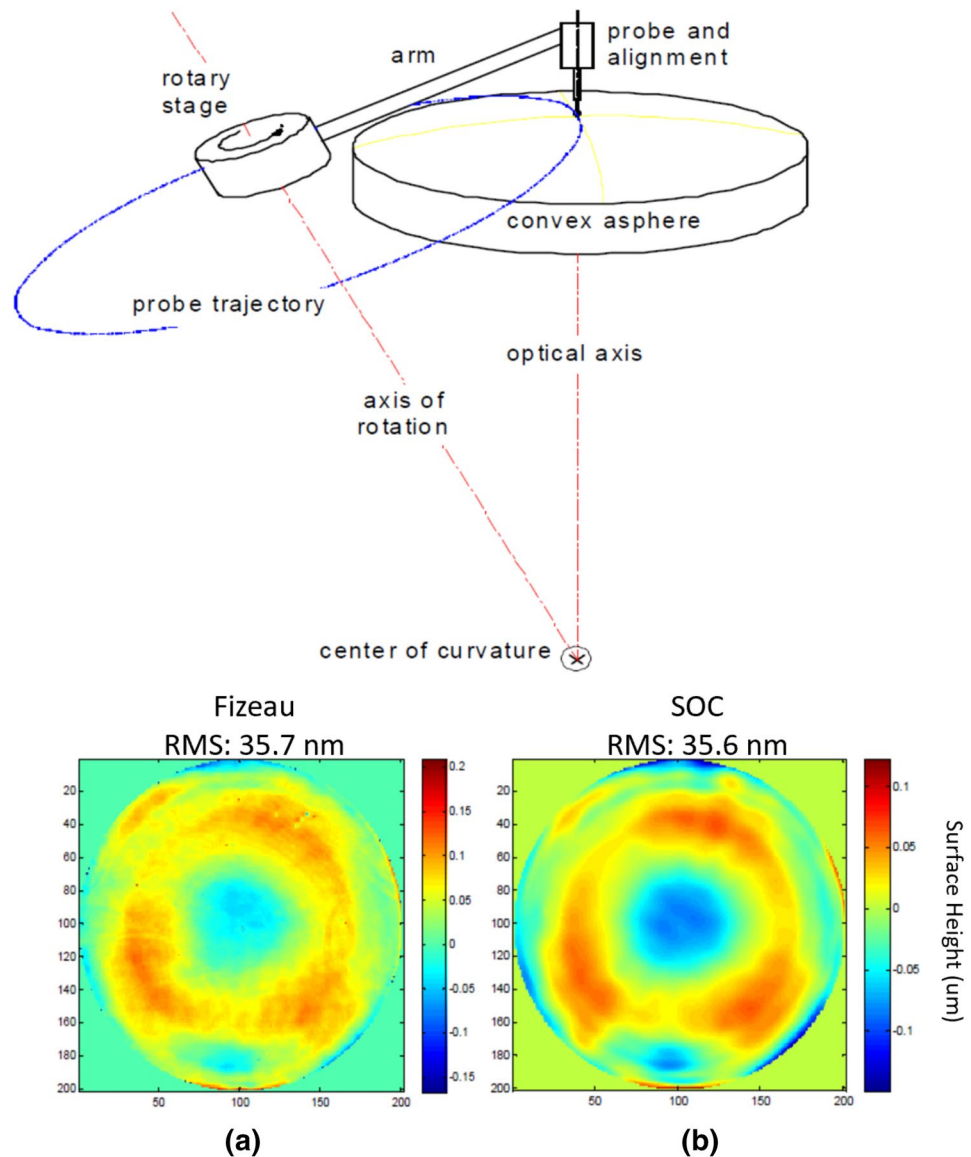
One approach to measuring surface figure error, particularly for rough surfaces, is using a swing arm profilometer (SAP). This technique uses a highly accurate probe which is mounted on a rotating arm such that its axis of rotation passes through the center of curvature of the tested optic [50]. The trajectory of the probe defines an arc that lies on a spherical surface defined by this center of curvature. The

test measures the optical surface departure from this spherical surface and is capable of testing convex, concave, and flat optical surfaces. With the next generation of extremely large telescope optics in mind a SAP was devised as a collaborative project between the University College London and the UK National Physical Laboratory and was able to achieve repeatability of 40 nm RMS using a touch probe and a high-resolution stage system [51]. Alternatively, a non-contact optical probe can be used in what is known as a Swing arm Optical Coordinate-measuring-machine (SOC) test, and has produced surface figure results comparable to a Fizeau Computer-Generated Hologram (CGH) interferometry test [52]. To achieve this, a dual probe shearing method is utilized to calibrate the system. The dual probe shear calibration approach is essential as the arm will have systematic errors from the arm bearing. Because both probes see the same bearing errors while measuring different areas of the test surfaces, the error can be calibrated out. Figure 15 demonstrates the SOC process as well as the accuracy of the SOC system as compared to a Fizeau test of a 1.4-m diameter aspheric surface with 300 μm of aspheric departure.

An interesting novel development which reverses the SAP concept has recently been reported, described as a Swinging Part Profilometer [53]. The concept is like the SAP, except instead of the probe swinging, the optic under test is placed on a rotation table and is rotated under the probe. One obvious benefit of a fixed probe is that the SAP method can be deployed for in situ metrology of a part during fabrication. The key requirement is that the optic is mounted on a rotary air-bearing or hydrostatic table, which would lend itself nicely to a CNC fabrication process. One challenge is that for lateral motion the optic must move while a counterweight maintains proper balance of the table. The method has successfully been applied to testing flat optical surfaces and was able to exceed the expected probe accuracy of 300 nm.

One final contact metrology method for rough surfaces is the utilization of a laser tracker [54]. A laser tracker is a device that uses two angular encoders and a distance-measuring interferometer (DMI) to measure the position of a retroreflector in 3 dimensions. DMIs offer excellent distance measurement capabilities, and significant research is constantly being performed to improve the technology. Recent advancements include utilizing mode-locked lasers for improved distance measurement performance [55]. To complement the laser tracker, and account for rigid body motion as well as air refractive index variations, the laser tracker metrology approach utilizes four independent DMIs which measure retroreflectors at the mirror edge continuously. In this way, the rigid body can be well defined, and the laser tracker position measurement can be calibrated. For the measurement itself, a spherically mounted retroreflector is moved via computer-controlled motion over the mirror and independent measurement points are taken across

Fig. 15 A swing arm profilometer (SAP) has been used to great success in measuring the surface form of several precision large optics (top). The method utilizes a probe tip, either optical or touch, which is swung over the optic under test. Simultaneously, the optic is rotated on a precision rotation table and the resulting acquired data is stitched together to form a full surface map. To demonstrate the capabilities of the method, a Fizeau test of an optic (a) was compared to an SAP test which used a dual probe shear calibration method (b). The Fizeau test data reported a surface RMS of 35.7 nm while the SOC (Swing arm Optical Coordinate-measuring-machine) reported 35.6 nm RMS. The direct subtraction shows a difference of only 9 nm RMS [52]



the full aperture. The points are then combined to form a surface map of the optic. For the first segment of the GMT telescope, the method was able to provide independent corroboration of low-order metrology results for the surface with accuracy exceeding 1 μm RMS.

For non-contact optical metrology of rough surfaces infrared-based deflectometry has recently been successfully integrated into the metrology plan of several of the optics in the NGTs as a rapid, high accuracy and high dynamic range non-null metrology method. Deflectometry fundamentally measures the deflection of a ray of light, which originates at a known source location, off of a test optic and onto a recording device such as a camera [56]. The technique is a non-null metrology method and has been utilized in measuring freeform optics [57]. For rough surfaces, a hot scanning source, such as a heated tungsten ribbon or heated ceramic

rod, provides radiation in the thermal-infrared spectrum that can specularly reflect from surfaces with roughness as high as 50 μm RMS [58]. The system was utilized in the DKIST fabrication and was able to greatly enhance the efficiency of fabrication, providing accurate metrology results during the grinding phase, which is often $\sim 1000\times$ faster removal process than the final polishing phase, by reporting surface figure error with a sampling of roughly 512×512 points across the 4.2-m surface down to below 1 μm of RMS departure from ideal [59]. A surface reconstruction from a deflectometry measurement taken during 40 μm grit loose abrasive grinding of a 6.5-m diameter mirror is shown in Fig. 16 and illustrates how the rough surface measurement capabilities of the technique.

Another non-contact method for testing large figure error of the base shape is a scanning pentaprism test [61]. This test

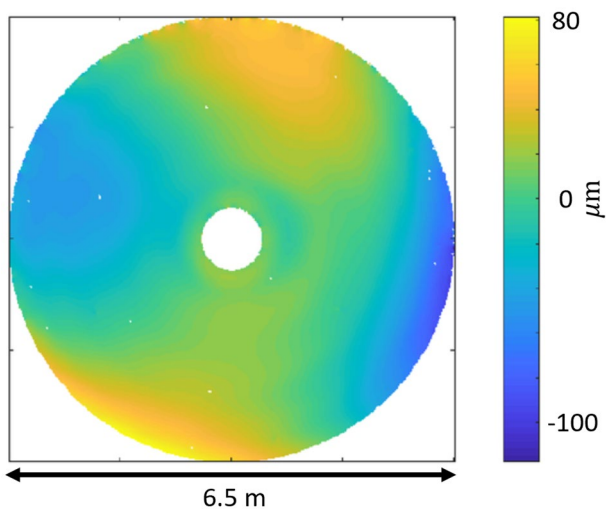


Fig. 16 The grinding phase of fabrication of an optic allows for extremely rapid convergence to the desired surface shape. Above, after grinding a 6.5-m optic with a 40- μm grit, the surface is tested with an improved infrared deflectometry system which uses a heated ceramic rod as the source and the surface map is reconstructed [60]

utilizes a pentaprism to scan a collimated beam across the optical test surface and measures the focus of the reflected beam. The technique has achieved slope accuracy down to 1 μrad RMS. Also, a novel method known as Exact Autocollimation Deflectometric Scanning (EADS) was able to achieve extremely high-precision measurement of surface slopes of a tested optic and shows great promise for measuring flat optics [62]. The method uses a null instrument which sends a signal through a scanning pentaprism to the optic surface. The optic itself sits on two points, one of which is a piezo-actuator, and the surface is tilted to achieve a null in the null instrument. Simultaneously, a mirror is mounted

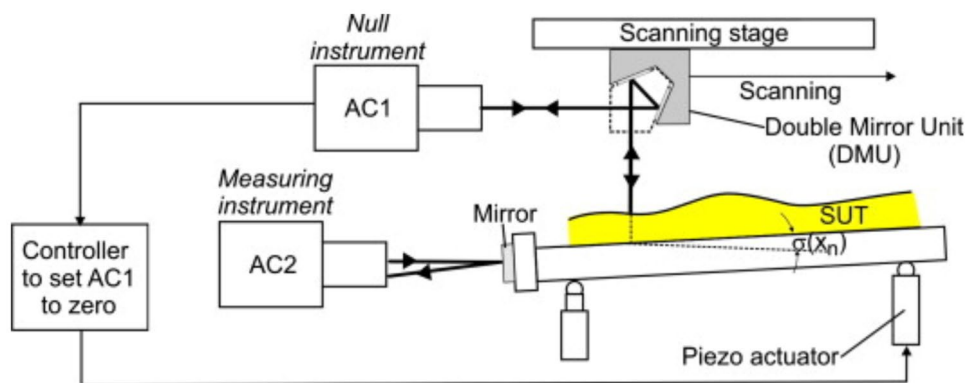


Fig. 17 Large flat mirrors are integral optical components in several of the NGTs. One method to achieve precision metrology of such surfaces is the EADS. The EADS principle utilizes a piezo-actuator to set the zero of AC1 (Autocollimator 1) at each position, while AC2 measures the precise slope. The system is able to achieve extreme precision for slope measurements and has been proposed to measure

perpendicular to the optic and reflects the tilt of the optical surface. An instrument measures the precise tilt of the mirror and the local slope of the optic can be determined to high accuracy. Figure 17 demonstrates the theory behind the testing method.

Moving toward smoother surfaces allows for more accurate optical metrology methods which operate in the visible spectrum to be utilized. One such method is Phase Shifting Deflectometry (PSD), which is similar to the infrared deflectometry mentioned earlier but adapted for improved visible-light performance. Instead of a heated scanning source, a digital screen is used to display a sinusoidal pattern which is phase shifted as a camera records the reflected images. This technique has been used in testing multiple large precision optics [56, 63, 64]. The setup for the concept is demonstrated in Fig. 18.

With careful calibration, PSD can extend metrology down to very fine surfaces, where interferometry excels. This has been demonstrated with 1 nm RMS surface height accuracy demonstrated with x-ray mirrors [65] and can achieve 300 nanoradian RMS slope precision [66]. Figure 19 demonstrates the acquisition and calibration process for a PSD system employed on a recently produced 6.5-m mirror, as well as the surface test results compared to an interferometric test.

The traditional fine-surface metrology technique of interferometry is undergoing improvements. One important area that has made great strides is subaperture stitching interferometry. This method is essential when testing large convex optics, which are featured in several next-generation telescope designs. Recently, a method which utilizes a reconfigurable null test was devised which utilizes a multi-axis platform and two rotating Computer-Generated Holograms (CGHs) to minimize systematic errors in subaperture

the flat mirrors used in large telescopes [62]. Reprinted from *Nuclear Instruments and Methods in Physics Research Section A: Accelerators, Spectrometers, Detectors and Associated Equipment*, Volume 710, M. Shulz, G. Ehret, P. Kren, *High accuracy flatness metrology within the European Metrology Research Program*, Pages 37–41., Copyright (2013), with permission from Elsevier

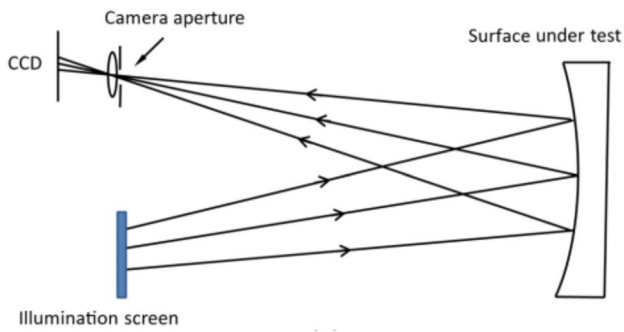


Fig. 18 Deflectometry has been used recently for metrology on several of the NGT optics, including the 4.2-m DKIST primary mirror and 8.4-m GMT primary mirror segments. The method uses a source which emits light at a known location. The light deflects from the optic under test and is recorded by a camera. By knowing the precise 3D location of all components, the local slope of the optic under test can be determined, and the surface sag is determined by integrating the local slopes [65]

measurements of a large convex asphere [68]. The acquisition and stitching process is demonstrated in Fig. 20.

For optics that are not highly convex one of the absolute best metrology results that can be achieved is via full

aperture high-precision interferometry. As interferometry is a null-test method, it requires a null configuration to obtain the best test results. This typically can be achieved by using an appropriate optic to null out the test optic; however, the process becomes more complicated for a freeform optic. To achieve the highest level of testing for freeform surfaces, using a custom Computer-Generated Hologram (CGH) is a commonly preferred method. Figure 21 demonstrates a custom CGH and the resulting fringe pattern.

One additional benefit of CGHs is that they can provide advanced alignment of the null configuration by utilizing additional alignment holograms outside of the main testing aperture of the CGH. Because the external references are generated at the same time as the main null pattern, they are aligned to the accuracy of the lithographic process that created the CGH [69]. The result is a better aligned, higher performance custom null configuration which can achieve extraordinary precision metrology of the freeform optics. It should be noted that even with the improved alignment and nulling features a CGH presents, the exact implementation for testing some of the described optics may introduce distortion in the interferometric setup which must be mapped

Fig. 19 Phase Shifting Deflectometry (PSD) and line scanning (a) are two common deflectometry source approaches. For the highest precision the geometry of the deflectometry test system is measured with a laser tracker (b) and fiducials are applied to the optic to map the camera distortion (c). Using this calibration approach, a PSD measurement (bottom left) achieved similar results to an interferometric measurement (bottom right) of a 6.5-m optic [67]

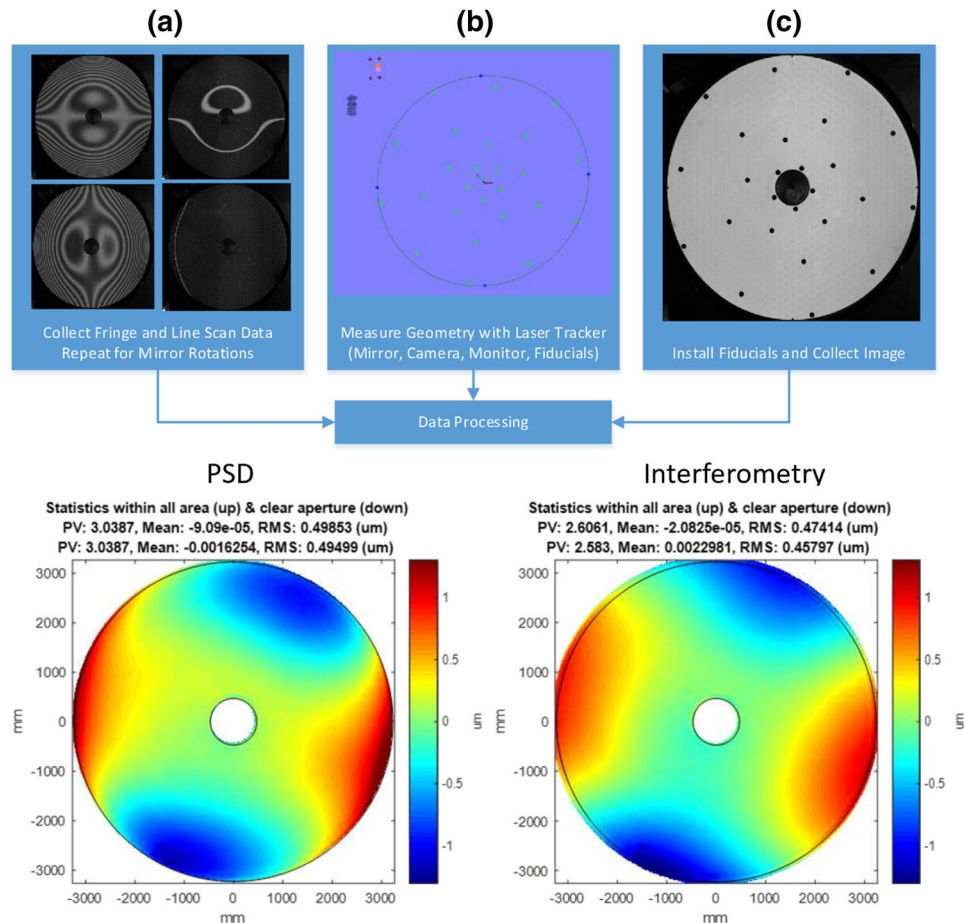


Fig. 20 Subaperture stitching interferometry allows for precise interferometric measurements of large surface that cannot be measured using a standard interferometric test. By utilizing a multi-axis platform to carefully adjust the measured subaperture (left) and counter-rotating CGHs (bottom right), a full map of the optic surface is obtained (top right). The subapertures are stitched, and system errors are calibrated out to produce a high-quality map [68] Reprinted from *Optics & Laser Technology*, Volume 91, S. Chen, S. Xue, Y. Dai, S. Li, *Subaperture stitching test of convex aspheres by using the reconfigurable optical null*, Pages 175–184., Copyright (2016), with permission from Elsevier

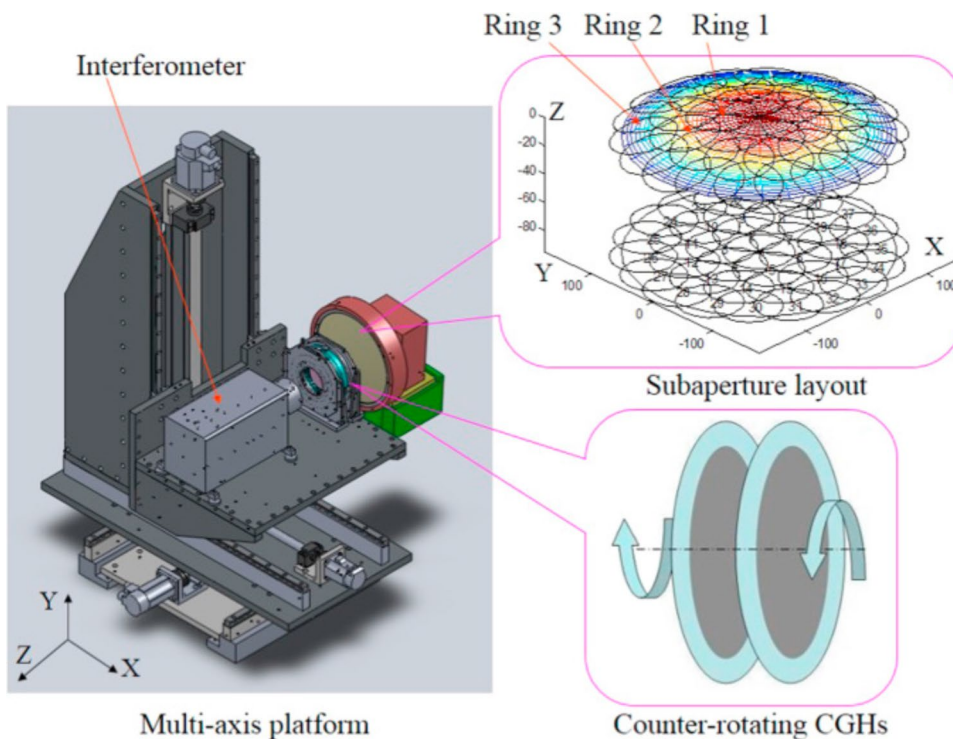
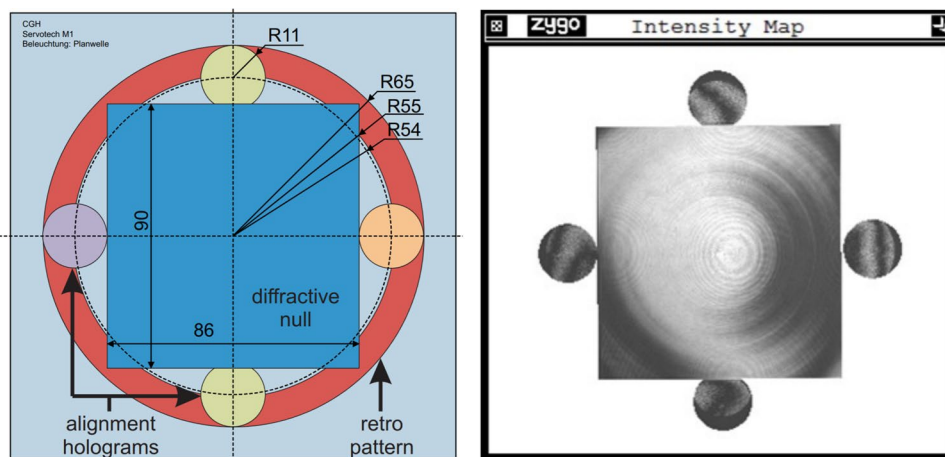


Fig. 21 For freeform optics, a custom null optic is required to achieve adequate fringe density over the entire optic aperture. A Computer-Generated Hologram (CGH) is an accurate way to generate extremely high-precision custom null optics and can feature helpful alignment features (left). When used, they can provide a proper fringe density for testing even over a highly freeform surface (right) [69]

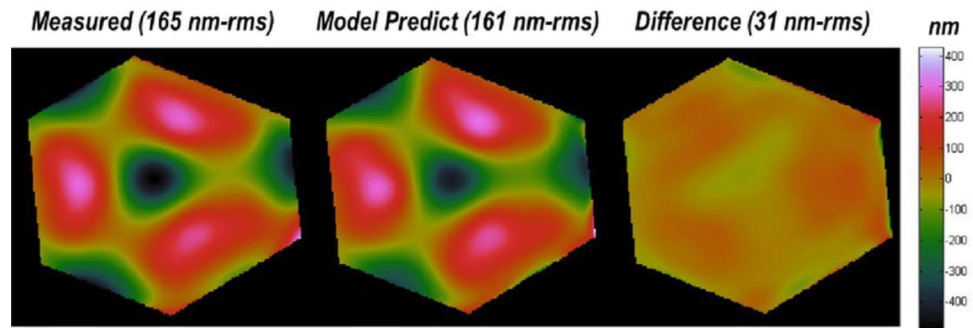


and calibrated to achieve a high accuracy metrology result [70].

Another metrology system that must be noted is the highly unique cryogenic center of curvature test system used for the JWST [71]. The test system consists of a multi-wavelength instantaneous interferometer, a calibration system, and a reflective null. Due to the long path length required for the center of curvature test, the instantaneous interferometry becomes

essential to eliminate random variations arising from vibrations, which with multiple tests can be averaged out. The system achieved a wavefront error (WFE) repeatability of 10.8 nm RMS. Figure 22 demonstrates the test results for a segment of the JWST using the cryogenic center of curvature test.

Fig. 22 The JWST mirror segments have extremely tight surface figure tolerances. Thus, a multi-wavelength instantaneous interferometer was an essential tool for measuring surface figure. The measured figure of one segment (left) is compared to a model-predicted surface (middle) and the difference of 31 nm RMS across the surface (right) was determined [71]



3.3 Large Primary Mirror Alignment and Co-phasing

Once the optics have been fabricated and meet specifications, they must be assembled and aligned. Not only must the mirrors be aligned relative to each other to create a well-aligned optical system, but for the segmented mirrors, co-phasing becomes essential. Additionally, proper alignment must be maintained throughout testing, where thermal gradients, gravity, and vibrations can cause small motions in the positions of the optics.

For systems such as the E-ELT and TMT, where there are hundreds of segments in the primary mirror, this alignment and co-phasing is a complex process. Because the steel structure which will support the optics is not sufficiently accurate to align the optics in these systems, additional interface structures, known as Fixed Frames in the E-ELT case, will be installed on top of the structure and aligned in six degrees of freedom to achieve the proper optical alignment [72]. The rigid fixturing is only the first step in the alignment for the large optics at play in these telescope systems. To get better performance active alignment and, in the case of segmented mirrors, co-phasing are required.

The TMT system uses an Alignment and Phasing System (APS) to control the 10,000+ degrees of freedom of the primary, secondary, and tertiary mirrors that constitute the system. The APS system, which is based on the Keck Telescope alignment system, is a Shack–Hartmann wavefront sensor which provides the pre-adaptive optics alignment for the TMT system [73]. The APS system adjusts the segment pistons and tip/tilts, the segment surface figure (by warping harness adjustments), the secondary mirror piston and tip/tilt, and the tilt and rotation of the tertiary mirror [74]. The typical test case for the system will be as follows: the telescope will be pointed at a star, the Acquisition Pointing and Tracking (ATP) camera will acquire the star, minor adjustments are made to center the star, and then the guiding process will begin. Based on the wavefront sensing, the system will then adjust the active position and phasing of the optics in the system.

The GMT primary segments have active control to correct figure, while the secondary segments have both active and adaptive control and can correct for phasing. Like the TMT, Shack–Hartmann sensors are used in conjunction with a guide star to determine mirror alignment, phasing, and shape error via ground-based adaptive optics. The design calls for a dispersed Hartmann design, with 1.5-m

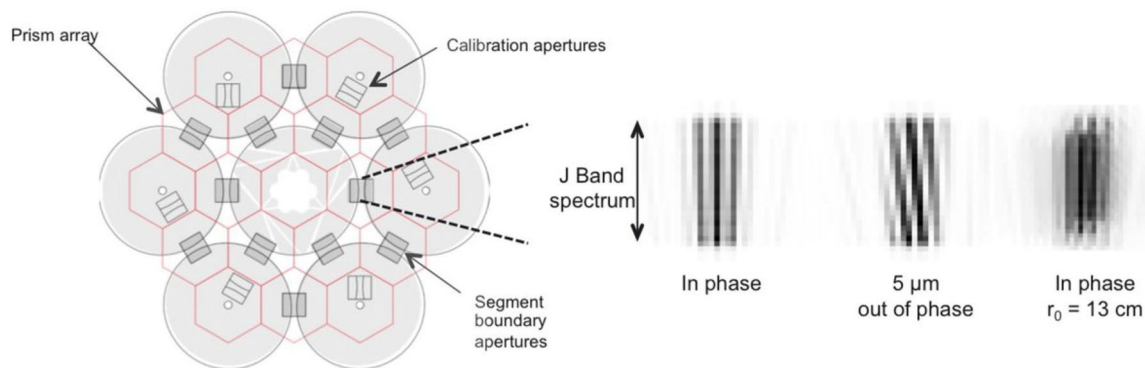


Fig. 23 The GMT, with its seven 8.4-m in diameter mirror segments (left), requires advanced mirror phasing to achieve proper alignment. The system will use a phasing camera system operating in the J band which, using dispersed fringes, will guide the phasing of the mirror

segments. When the mirrors are properly in phase a correct fringe pattern is achieved. The out of phase error is reflected in the fringe pattern by tilted fringes, allowing the system to correctly guide the mirrors to proper phasing. r_0 represents median Fried parameter [17]

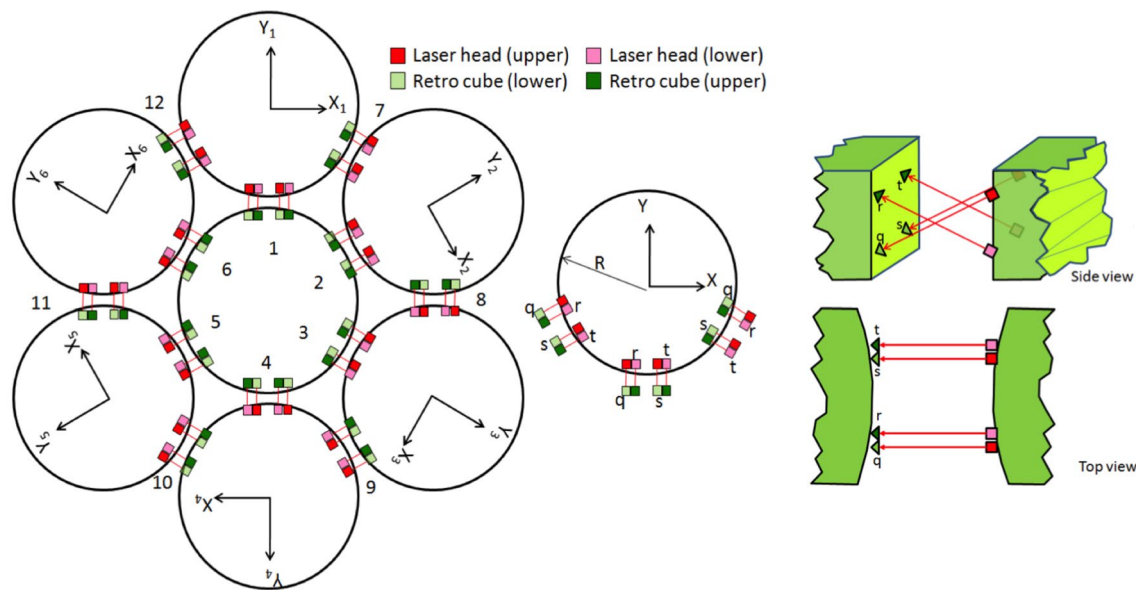


Fig. 24 The primary mirror of the GMT has seven segments that must be properly aligned to each other to within 10 nm. To accomplish this, distance-measuring interferometers (DMIs) will be used to monitor the positioning of the mirrors during operations and will

square apertures arranged at the tangent of each segment [75, 76]. These apertures create interference fringes, which are measured by a Dispersed Fringe Sensor (DFS) in an infrared channel. The patterns are recorded in the J band (1050–1350 nm) over a short integration time (10–20 ms) using a SAPHIRA eAPD array. This approach will be used to achieve optical path differences of less than 85 nm RMS between segments [17]. Figure 23 demonstrates the fringe phasing concept. After this step, a pyramid-based natural guide-star wavefront sensor (NGWS) will be used and can control piston to within 30 nm RMS.

To measure the position of the primary segments during observations an interferometric metrology system will be used. Distance-measuring interferometers will be used in 24 pairs to measure distance shifts of 5 nm but also are able to measure large motions during initial alignment of up to 3 cm. A similar network of distance-measuring interferometers will be used to monitor the alignment of the secondary mirror segments. Figure 24 illustrates the geometry of the laser truss at $M1$.

3.4 Active and Adaptive Optics Control

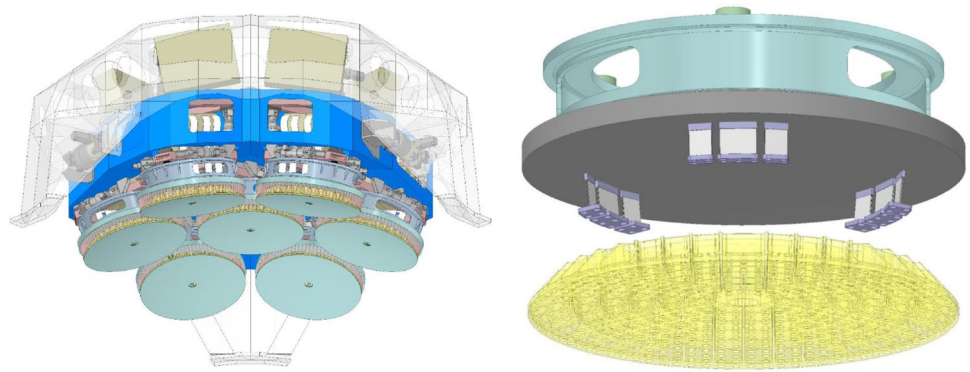
While the complex optical designs allow for extremely high-quality imaging and superb light-collecting capabilities, both active and, for ground-based systems, adaptive optics are required to achieve the desired system performance of these telescopes. This need is answered in an equally diverse set

of methods as the optical design choices for the systems described. It must be considered as well that while some systems, such as the DKIST or LSST, have very specific science goals, the extremely large telescope systems have a wide variety of different observation goals and thus require a variety of different observing modes. Because of this, all the systems require advanced positioning control for slower shifts and mechanical drift. This control is provided by the active optics in the system.

On the other hand, for the ground-based telescopes, atmosphere-induced aberrations must also be controlled, or the imaging capabilities would be severely limited. This presents an interesting problem, as with increasingly large mirror areas the feasibility of adaptive optics covering such areas becomes challenging. Thus, a greater variation in design choices arises with the adaptive optics approach, whether they are implemented in the secondary mirror as is the case in the GMT, or in final stage deformable mirrors, as is the case in the E-ELT, TMT, and DKIST. To enable adaptive systems, a method is required for determining the wavefront that must be corrected. This is increasingly being accomplished using extremely powerful sodium guide-star lasers which create an ideal guide star. Similarly, while certain unique choices have been made to create highly accurate wavefront sensors, the base theory still mostly relies on Shack–Hartmann sensors. However, the exact implementation of the wavefront sensors is typically unique to the

guide correction of position. The DMIs use a laser which is reflected by a retro cube to measure distance to within 5.9 nm RMS and to ~ 0.01 μ rad in tilt [77]

Fig. 25 The GMT secondary mirror makes use of seven paired segments (left), which are mounted into a Zerodur reference body. The secondary mirror segments are complementary to the primary segments and can be actively driven. Additionally, a suite of actuators provides adaptive control to the secondary mirror segments (right) [17]



telescope requirements, as seen in the curvature wavefront sensor implemented for the LSST [78].

While a number of the NGTs utilize a flat deformable mirror either near the end of the optical train or integrated into the science instruments, the GMT instead uses an adaptive secondary mirror. The GMT secondary will provide both active optics and adaptive optics. Because these two systems were designed in conjunction for the GMT, they broadly fall under the wavefront control (WFC) system [17]. Figure 25 demonstrates the mount for the GMT secondary segments. Included in the system are four distinct wavefront control modes.

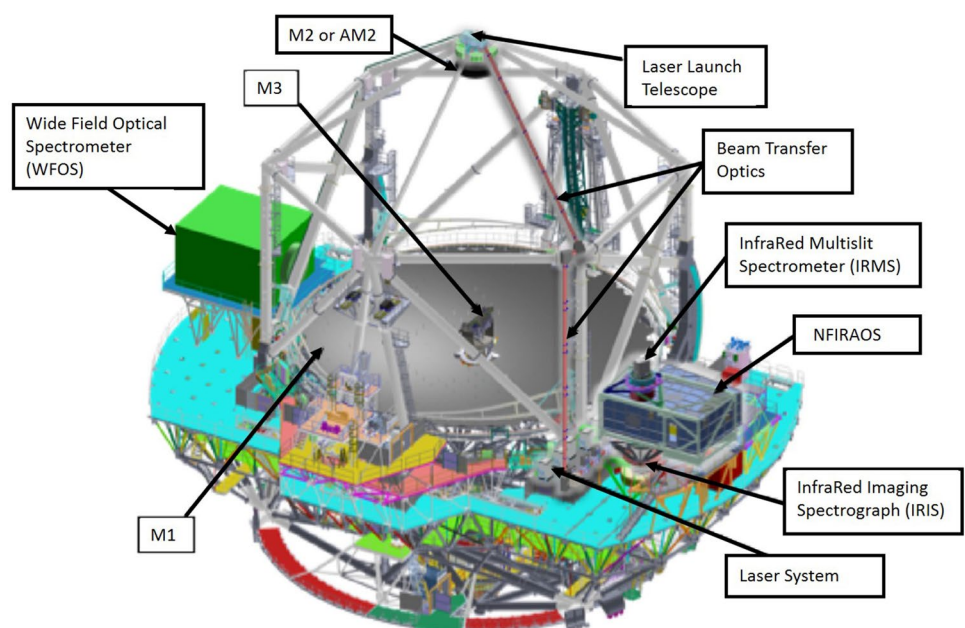
The ground layer AO observing mode requires active control of the primary mirror ($M1$) segment positions and figure with fast (100 Hz) control of the secondary mirror ($M2$) figure. Because each of the seven primary segments is matched to a segment of the secondary mirror, active positioning control of the $M2$ segments can directly compensate $M1$ position errors. Additionally, a natural guide star observing

mode will deliver a high contrast, diffraction-limited Point Spread Function (PSF) in the near-infrared. Finally, laser tomography adaptive optics can be used to reconstruct the high-order components of the atmospheric wavefront error in the direction of faint on-axis targets.

Four general-purpose natural guide-star wavefront-sensing probes located 450 mm ahead of the direct Gregorian focus provide the feedback for the natural seeing and GLAO observing modes. The diffraction-limited natural guide star and laser tomography observing modes require additional wavefront sensors in the instruments. Each diffraction-limited instrument is therefore equipped with a pyramid wavefront sensor for use when a bright natural guide star is available, and a set of 6 Shack–Hartmann wavefront sensors for use with a constellation of laser guide stars.

The TMT also is planning to make use of an adaptive secondary mirror [18]. Plans have investigated using a single Adaptive $M2$ (AM2) mirror that acts as a ground-based adaptive optic system. This design choice would allow for

Fig. 26 Adaptive optics control is essential for the observations performed by the NGTs. After extremely precise manufacturing and alignment, constant adaption of the optical system to atmospheric turbulence and other motions (gravity, wind, etc.) must be performed to maintain the system requirements. The TMT system will utilize adaptive optics in the steering mirrors and inside of the instruments on the Nasmyth stations. Additionally, a laser launch telescope will be used to produce a laser guide star, using powerful sodium lasers [18]



a simplification in the instrument adaptive optics. Although the adaptive $M2$ is in a planning stage, there is a suite of other adaptive optical control systems that will be utilized. The adaptive optics system itself is heavily incorporated into the primary instrument for the TMT, the Narrow Field IR Adaptive Optics System (NFIRAOS). The system utilizes a series of advanced wavefront sensors and deformable mirrors and a separate guide laser system. The guide laser will be composed of six 25 W sodium lasers, which will be Raman Fiber lasers that utilize second harmonic generation to achieve 598 nm output. Such lasers allow for high output, high reliability, and strong interface with the adaptive optics system in the NFIRAOS. Figure 26 demonstrates the wavefront correction suite that will be incorporated into the TMT telescope.

4 Next-Generation Observatories

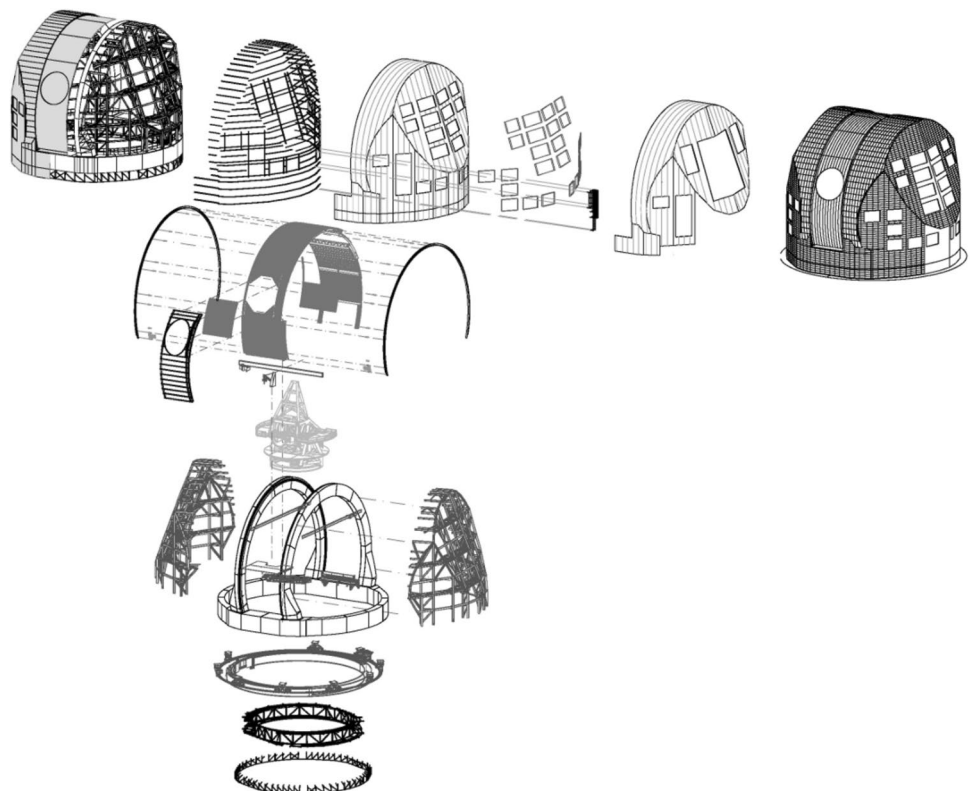
4.1 Enclosure Design

The NGTs are incorporating larger systems with greater precision requirements than ever before in history. The ground-based systems require housing that is larger than any previous telescope system enclosures, with some structure being of a similar scale as a large sport stadium. Additionally,

they require high precision and accuracy in alignment in azimuthal and altitudinal pointing while providing excellent stray light control. To minimize atmospheric losses, the ground-based NGTs are being installed primarily at very high altitudes and require wind control mechanisms to minimize wind-induced vibrations, as well as methods to control for earthquake-induced movements. Finally, the tracking and movement speeds for these systems are expected to operate at the same or higher rates as the current generation of smaller telescopes. To accommodate these requirements, novel design choices have been made for the enclosure systems of these telescopes [20].

One novel aspect in many of the newer telescopes is managing a wider field of view. This requirement demands unique optical designs and configurations, as well as new enclosure choices to provide the required viewing aperture for the telescope optics while still providing the required protection. For example, the LSST, with its 8.4-m diameter primary mirror and wide field of view (3.5°), is particularly susceptible to stray light and requires a unique design to mitigate the issue while also balancing wind-induced vibrations [79]. To accommodate wind vibration and stray light management the enclosure incorporates a rotating wind-screen as well as a light baffle system. The windscreen itself operates as a light screen and helps to define a clear aperture for viewing. All vents include a light baffle system and will provide dome flushing to minimize air turbulence inside of

Fig. 27 The DKIST enclosure required a unique mechanism to accurately and quickly track the Sun. The main aperture is guided using a crawler system, which offers greater precision and speed in movement. To maintain structural rigidity over the motion two twin arches are used to support the crawler system. Further, the azimuthal pointing is controlled using a rotating ring which the entire enclosure is mounted on top of [80]



the enclosure. Additionally, the system is expected to operate continuously without rotational travel limits. To accommodate this requirement, the Azimuth drives for the system are in the lower enclosure, which allows for glycol water cooling without the need for a utility cable wrap. Lastly, temperature conditioning during daytime use will be controlled via an air vent which aligns with the dome in the parked position.

While the LSST requires a large, unrestricted field of view and excellent stray light control, the DKIST requires a highly precise aperture and tracking mechanism to meet the 0.03 arcsec visible solar imaging resolution laid out in its science mission. The telescope will soon be providing unprecedented observations of the Sun at the Haleakala High Altitude Observatory in Maui, Hawaii. Due to its mission of performing fine detailed solar observations, there are unique requirements placed on the dome enclosure design for the DKIST system, which is 22 m in height and 26.6 m in diameter [21]. Figure 27 demonstrates the various components in the support and steering systems that make up the enclosure.

Perhaps the most unique design feature in the DKIST enclosure is the method used to position the system's first aperture stop. This aperture stop must track the Sun to high accuracy and provide a clear viewing aperture while precisely controlling stray light. Because of the speed and accuracy required to precisely track the Sun a more traditional aperture system was ruled out for the telescope. Instead, the shutter system for the DKIST telescope utilizes a crawler type system, which achieves positioning accuracy with a maximum tracking velocity of $0.75^\circ/\text{s}$ [80]. Further, the crawler system will always have several teeth in contact with the gearing system that controls movement, assuring steady and reliable tracking motion of the aperture. Due to the high thermal load placed on the system, the aperture shutter was designed to be actively water cooled. The shutter system itself is reinforced to accommodate varying gravitational loads based on the position. To maintain the required position accuracy, the altitude positioning system, via the crawler mechanism, is supported by two arch girders which provide high torsional strength and are further strengthened by the secondary structure. The arch girders are attached to a base ring, which is a key component for the azimuthal pointing system.

One final area that has introduced major design innovations in enclosures is that of extremely large telescopes. Due to the large aperture area required to permit light into the telescopes and the sheer size of these structures various new practices have been developed. The GMT enclosure takes a novel approach to the shutter concept for the system. The enclosure utilizes vertical shutter doors which can open and close depending on the activity of the telescope. For the vertical region, a horizontally sliding segment can retract

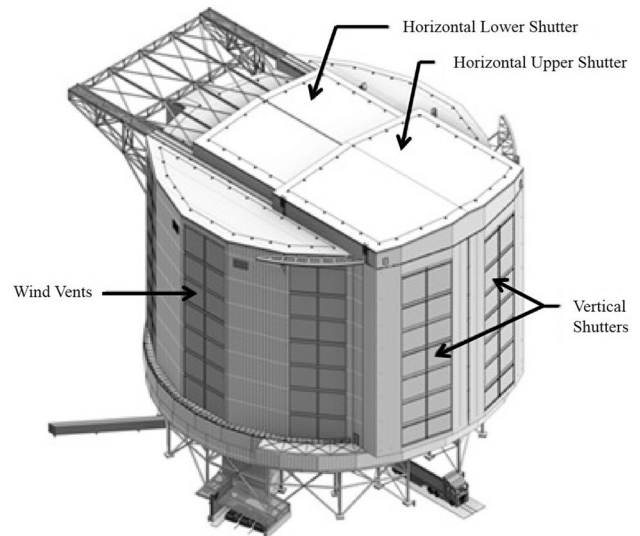


Fig. 28 The GMT enclosure departs from a dome shape in part due to the extreme size of the enclosure and the required shutter opening area. Instead, twin vertical shutters will slide horizontally to open the system while a top horizontal shutter will open as well. A deployable windscreen can also be used to minimize wind effects [81]



Fig. 29 The E-ELT enclosure will be a super-massive structure which houses the 40-m telescope. The structure currently is designed as a hemispherical dome with two sliding doors that will open the telescope to the night skies. The entire dome rests on a circular track which will allow for rotation of the enclosure. Due to the enormous size, multiple support structures are planned to maintain the required stiffness and positioning accuracy of all components [83]

to open the telescope to the night skies. A vertically sliding windscreen can also be deployed when the shutter is open, and the enclosure will have a robust seismic isolation system [81]. Figure 28 demonstrates a model of the proposed enclosure for the GMT system.

The E-ELT takes a different approach to the shutter requirement. While it too will make use of two horizontally

sliding twin doors to create a shutter, the enclosure is a more traditional dome design, and the vast shutter doors structure will slide apart to open the aperture [82]. Beyond that, the E-ELT will require a seismic isolation system to isolate the telescope system from any seismic vibrations. The dome itself is a hemispherical shape which rests upon a track which allows for rotation. The rotating enclosure will weigh 5500 tons and requires multiple support arches and structures [83]. Figure 29 displays the projected final dome design for the E-ELT.

4.2 Observatory Locations

The locations of the NGT observatories place significant demands on the structure designs. Despite the challenges, however, these exceptional sites provide key conditions essential for the observatories to accomplish their scientific goals. In order to increase the useful on-sky time for the next generation of ground-based telescopes, site selections must consider weather patterns in a changing climate (to minimize cloudy nights), minimize present and future light pollution from nearby cities, consider atmospheric turbulence that compromises image quality, and—for infrared observations—seek to minimize atmospheric water vapor content due to water's strong absorption bands. Thus, we see a preference for remote, mountainous deserts. With these considerations in mind, most of the next generation of telescopes will be located either on the summits of mountains in Hawaii or Chile.

The GMT system will be located at Las Campanas Observatory and the E-ELT in Cerro Armazones in Chile [84]. These sites have some defining features that make them ideal sites for observatories. Namely, the observatories are at the summits of tall but accessible mountains, thus reducing light pollution and creating a situation where there is less atmospheric interference between the telescope and space. Key parameters that were considered when selecting these locations, and the specific position inside the observatory area, were the cloud cover index and the frequency of achieving photometric sky conditions, as well as spectroscopic sky conditions. Additionally, wind speeds are low enough that the telescopes will be able to remain open to observations for a significant amount of time, while temperature is quite stable, and humidity is ideally low. Perhaps most important, however, is the precipitable water vapor (PWV) characteristics. The goal is to have low PWV values which are stable over the night [85].

The TMT is planning to build on Mauna Kea in Hawaii [86]. Like Cerro Campanas, the summit of Mauna Kea offers the required wind, humidity, and light levels for the observatories to maximize their scientific capabilities. The DKIST telescope construction is well underway on the Haleakala in

Hawaii, which has access to quality infrastructure benefiting the construction process [87].

5 Concluding Remarks

The next generation of telescopes promise to be key enablers for future discoveries in astronomy. To achieve the required performance, novel design choices and improvements are being made at all levels of the telescopes. The new norm for optics used in the NGTs are those of extremely large freeform surfaces, with some systems such as the LSST and GMT utilizing monolithic mirror segments up to 8.4-m in diameter, and others with numerous 1.5-m sized segments. The scope of the primary mirrors has defined a new subset of telescopes, known as extremely large telescopes, whose primary mirror diameters can range up to 40 m.

The size of these optics and the tolerances required have demanded novel ultra-precise and efficient fabrication methods. From utilizing rapid CNC machining processes and diamond-turned optics with precise grinding and polishing techniques, the fabrication methods are producing more accurate surfaces over a wider range of freeform shapes. To verify the surfaces created and guide the fabrication process, novel and improved metrology methods have been developed. For example, deflectometry has begun to be used in a variety of different ways to provide metrology from the grinding phase through to micro-finish measurements. Additionally, improvements in interferometry have led to better results when performing subaperture measurements, an essential technique for quantifying convex optics, as well as improved interferometric methods which utilize CGHs for nulling and alignment. With these methods, the most accurate, freeform, and largest optics ever produced are now being put together to create the next generation of telescopes.

The work does not end after fabrication. Complex structures and enclosures are necessary to assure proper alignment of the optics, as well as tracking capabilities. The enclosures must provide light baffling and prevent wind or seismic events from disrupting or damaging the optics. This has driven the extremely large telescope systems to explore shutters which slide horizontally to accommodate the vast shutter areas required. Due to entirely different design requirements calling for high speed, high accuracy aperture positions, the DKIST telescope uses a more traditional circular aperture driven by a novel crawler system to meet stringent accuracy and tracking speed requirements.

Finally, once the telescopes have been installed in their structures, they will undergo active and adaptive optical control to achieve the best possible results. The active control of optics will allow for accurate mirror alignment throughout observation and can utilize phasing measurements to

assure all segmented mirrors are appropriately aligned and co-phased throughout operation. The adaptive optics, for ground-based systems, will greatly improve optical performance by compensating atmospheric-induced aberrations using high-frequency corrections, allowing for near diffraction-limited performance for these systems.

When the next generation of telescopes goes on-line, with some planning to begin operations as early as 2019, astronomers will have access to an unprecedented amount of detailed scientific information. These instruments promise to provide a look farther back in time, provide greater resolution, wider fields of view, and more detailed data acquisition. Further, they will work in conjunction with not only each other but the existing telescope systems to complement one another. We now must wait and watch as these super-instruments complete the final steps in their complex and long development process before they begin producing scientific results.

Acknowledgements We would like to thank Antonin Bouchez for his expert input to the paper's adaptive and active optics section. Also, this review and summary work was made possible in part by the II-VI Foundation Block-Gift Program, the Technology Research Initiative Fund Optics/Imaging Program, the Korea Basic Science Institute Foundation, and the Friends of Tucson Optics Endowed Scholarships in Optical Sciences.

References

- Bernstein R, Dressler A, Apai D, Asplund M, Blum R, Brough S, Crane J, Cypriano E, Eisenstein D, Eisner J, Fabricant D, Gladders M, Greene J, Hwang N, Krause A, Papovich C, Sharp R, Simcoe R, Zaritsky D (2018) GMT Science Book 2018. Giant Magellan Telescope. GMTO, Vallenar
- European Southern Observatory (2010) An expanded view of the universe: science with the European Extremely Large Telescope. Garching bei München, Germany, European Southern Observatory
- King HC (1955) The history of the telescope. Griffin, London
- Fanson J, McCarthy PJ, Bernstein R, Angeli G, Ashby D, Bigelow B, Bouchez A, Burgett W, Chauvin E, Contos A, Figueroa F, Gray P, Groark F, Laskin R, Millan-Gabet R, Rakich A, Sandoval R, Pi M, Wheeler N (2018) Overview and status of the Giant Magellan Telescope project. In: Ground-based and airborne telescopes VII. Presented at the ground-based and airborne telescopes VII, international society for optics and photonics, p 1070012. <https://doi.org/10.1117/12.2313340>
- Martins CJAP, Leite ACO, Pedrosa POJ (2014) Fundamental cosmology with the E-ELT. *Proc Int Astron Union* 10:385–387. <https://doi.org/10.1017/S1743921314013441>
- Skidmore W, Anupama GC, Srianand R (2018) The Thirty Meter Telescope International Observatory facilitating transformative astrophysical science. [arXiv:1806.02481\[astro-ph\]](https://arxiv.org/abs/1806.02481)
- Skidmore W (2015) Thirty Meter Telescope detailed science case: 2015. *Res Astron Astrophys* 15:1945. <https://doi.org/10.1088/1674-4527/15/12/001>
- Rudnick L, NASA, JPL-Caltech (2006) Lighting up a dead star's layers. NASA Spitzer Space Telescope. <http://www.spitzer.caltech.edu/images/1675-ssc2006-19a-Lighting-up-a-Dead-Star-s-Layers>. Accessed 8 Oct 2018
- Tamai R, Spyromilio J (2014) European extremely large telescope: progress report. In: Ground-based and airborne telescopes V. Presented at the ground-based and airborne telescopes V, international society for optics and photonics, p 91451E. <https://doi.org/10.1117/12.2058467>
- Tamai R, Cerasuolo M, González JC, Koehler B, Tuti M (2016) The E-ELT program status. In: Ground-based and airborne telescopes VI. Presented at the ground-based and airborne telescopes VI, international society for optics and photonics, p 99060W. <https://doi.org/10.1117/12.2232690>
- Lightsey PA, Atkinson CB, Clampin MC, Feinberg LD (2012) James Webb Space Telescope: large deployable cryogenic telescope in space. *OE, OPEGAR* 51:011003. <https://doi.org/10.1117/1.OE.51.1.011003>
- Ivezić Ž, Kahn SM, Tyson JA, Abel B, Acosta E, Allsman R, Alonso D, AlSayyad Y, Anderson SF, Andrew J, Angel JRP, Angeli GZ, Ansari R, Antilogus P, Araujo C, Armstrong R, Arndt KT, Astier P, Aubourg É, Auza N, Axelrod TS, Bard DJ, Barr JD, Barrau A, Bartlett JG, Bauer AE, Bauman BJ, Baumont S, Becker AC, Becla J, Beldica C, Bellavia S, Bianco FB, Biswas R, Blanc G, Blazek J, Blandford RD, Bloom JS, Bogart J, Bond TW, Borgland AW, Borne K, Bosch JF, Boutigny D, Brackett CA, Bradshaw A, Brandt WN, Brown ME, Bullock JS, Burchat P, Burke DL, Cagnoli G, Calabrese D, Callahan S, Callen AL, Chandrasekharan S, Charles-Emerson G, Chesley S, Cheu EC, Chiang H-F, Chiang J, Chirino C, Chow D, Ciardi DR, Claver CF, Cohen-Tanugi J, Cockrum JJ, Coles R, Connolly AJ, Cook KH, Cooray A, Covey KR, Cribbs C, Cui W, Cutri R, Daly PN, Daniel SF, Daruich F, Daubard G, Daus G, Dawson W, Delgado F, Dellapenna A, de Peyster R, de Val-Borro M, Digel SW, Doherty P, Dubois R, Dubois-Felsmann GP, Durech J, Economou F, Eracleous M, Ferguson H, Figueroa E, Fisher-Levine M, Focke W, Foss MD, Frank J, Freeman MD, Gangler E, Gawiser E, Geary JC, Gee P, Geha M, Gessner CJB, Gibson RR, Gilmore DK, Glanzman T, Glick W, Goldina T, Goldstein DA, Goodenow I, Graham ML, Gressler WJ, Gris P, Guy LP, Guyonnet A, Haller G, Harris R, Hascall PA, Haupt J, Hernandez F, Herrmann S, Hileman E, Hoblitt J, Hodgson JA, Hogan C, Huang D, Huffer ME, Ingraham P, Innes WR, Jacoby SH, Jain B, Jammes F, Jee J, Jenness T, Jernigan G, Jevremović D, Johns K, Johnson AS, Johnson MWG, Jones RL, Juramy-Gilles C, Jurić M, Kalirai JS, Kallivayalil NJ, Kalmbach B, Kantor JP, Karst P, Kasliwal MM, Kelly H, Kessler R, Kinnison V, Kirkby D, Knox L, Kotov IV, Krabbendam VL, Krughoff KS, Kubánek P, Kuczewski J, Kulkarni S, Ku J, Kurita NR, Lage CS, Lambert R, Lange T, Langton JB, Guillou LL, Levine D, Liang M, Lim K-T, Lintott CJ, Long KE, Lopez M, Lotz PJ, Lupton RH, Lust NB, MacArthur LA, Mahabal A, Mandelbaum R, Marsh DS, Marshall PJ, Marshall S, May M, McKecher R, McQueen M, Meyers J, Migliore M, Miller M, Mills DJ, Miraval C, Moeyens J, Monet DG, Moniez M, Monkewitz S, Montgomery C, Mueller F, Muller GP, Arancibia FM, Neill DR, Newbry SP, Nief J-Y, Nomerotski A, Nordby M, O'Connor P, Oliver J, Olivier SS, Olsen K, O'Mullane W, Ortiz S, Osier S, Owen RE, Pain R, Palecek PE, Parejko JK, Parsons JB, Pease NM, Peterson JM, Peterson JR, Petravick DL, Petrick MEL, Petry CE, Pierfederici F, Pietrowicz S, Pike R, Pinto PA, Plante R, Plate S, Price PA, Prouza M, Radeka V, Rajagopal J, Rasmussen AP, Regnault N, Reil KA, Reiss DJ, Reuter MA, Ridgway ST, Riot VJ, Ritz S, Robinson S, Roby W, Roodman A, Rosing W, Roucelle C, Rumore MR, Russo S, Saha A, Sassolas B, Schalk TL, Schellart P, Schindler RH, Schmidt S, Schneider DP, Schneider MD, Schoening W, Schumacher G, Schwamb ME, Sebag J, Selvy B, Sembroski GH, Seppala LG, Serio A, Serrano E, Shaw RA, Shipsey I, Sick J, Silvestri N, Slater CT, Smith JA, Smith RC, Sobhani S, Soldahl

- C, Storrie-Lombardi L, Stover E, Strauss MA, Street RA, Stubbs CW, Sullivan IS, Sweeney D, Swinbank JD, Szalay A, Takacs P, Tether SA, Thaler JJ, Thayer JG, Thomas S, Thukral V, Tice J, Trilling DE, Turri M, Van Berg R, Berk DV, Vetter K, Virieux F, Vucina T, Wahl W, Walkowicz L, Walsh B, Walter CW, Wang DL, Wang S-Y, Warner M, Wiecha O, Willman B, Winters SE, Wittman D, Wolff SC, Wood-Vasey WM, Wu X, Xin B, Yoachim P, Zhan H, Collaboration for the L (2008) LSST: from science drivers to reference design and anticipated data products. *arXiv:0805.2366[astro-ph]*
13. Sassolas B, Teillon J, Flaminio R, Michel C, Morgado N, Pinard L (2013) Development on large band-pass filters for the wide field survey telescope LSST. In: *Optical interference coatings (2013)*, paper MD.2. Presented at the optical interference coatings, optical society of America, MD.2. <https://doi.org/10.1364/OIC.2013.MD.2>
 14. Martin HM, Angel JRP, Angeli GZ, Burge JH, Gressler W, Kim DW, Kingsley JS, Law K, Liang M, Neill D, Sebag J, Strittmatter PA, Tuell MT, West SC, Woolf NJ, Xin B (2016) Manufacture and final tests of the LSST monolithic primary/tertiary mirror. In: *Advances in optical and mechanical technologies for telescopes and instrumentation II*. Presented at the advances in optical and mechanical technologies for telescopes and instrumentation II, international society for optics and photonics, p 99120X. <https://doi.org/10.1117/12.2234501>
 15. Callahan S, Gressler W, Thomas SJ, Gessner C, Warner M, Barr J, Lotz PJ, Schumacher G, Wiecha O, Angeli G, Andrew J, Claver C, Schoening B, Sebag J, Krabbendam V, Neill D, Hileman E, Muller G, Araujo C, Martinez AO, Aguado MP, García-Marchena L, Argandoña IR, de Romero FM, Rodríguez R, González JC, Venturini M (2016) Large Synoptic Survey Telescope mount final design. In: *Ground-based and airborne telescopes VI*. Presented at the ground-based and airborne telescopes VI, international society for optics and photonics, p 99060M. <https://doi.org/10.1117/12.2232996>
 16. Tritschler A, Rimmele TR, Berukoff S, Casini R, Kuhn JR, Lin H, Rast MP, McMullin JP, Schmidt W, Wöger F, Team D (2016) Daniel K. Inouye Solar Telescope: high-resolution observing of the dynamic Sun. *Astron Nachr* 337:1064–1069. <https://doi.org/10.1002/asna.201612434>
 17. Bouchez AH, Angeli GZ, Ashby DS, Bernier R, Conan R, McLeod BA, Quirós-Pacheco F, van Dam MA (2018) An overview and status of GMT active and adaptive optics. In: *Adaptive optics systems VI*. Presented at the adaptive optics systems VI, international society for optics and photonics, p 107030W. <https://doi.org/10.1117/12.2314255>
 18. Boyer C (2018) Adaptive optics program at TMT. In: *Adaptive optics systems VI*. Presented at the adaptive optics systems VI, international society for optics and photonics, p 107030Y. <https://doi.org/10.1117/12.2313753>
 19. Perrin MD, Acton DS, Lajoie C-P, Knight JS, Lallo MD, Allen M, Baggett W, Barker E, Comeau T, Coppock E, Dean BH, Hartig G, Hayden WL, Jordan M, Jurling A, Kulp T, Long J, McElwain MW, Meza L, Nelan EP, Soummer R, Stansberry J, Stark C, Telfer R, Welsh AL, Zielinski TP, Zimmerman NT (2016) Preparing for JWST wavefront sensing and control operations. In: *Space telescopes and instrumentation 2016: optical, infrared, and millimeter wave*. Presented at the space telescopes and instrumentation 2016: optical, infrared, and millimeter wave, international society for optics and photonics, p 99040F. <https://doi.org/10.1117/12.2233104>
 20. Murga G, Bilbao A, de Bilbao L, Lorentz TE (2016) Design solutions for dome and main structure (mount) of giant telescopes. In: *Ground-based and airborne telescopes VI*. Presented at the ground-based and airborne telescopes VI, international society for optics and photonics, p 99060C. <https://doi.org/10.1117/12.2233502>
 21. Murga G, Marshall HK, Lorentz TE, Ariño J, Ampuero P (2014) DKIST enclosure fabrication factory assembly and testing. In: *Ground-based and airborne telescopes V*. Presented at the ground-based and airborne telescopes V, international society for optics and photonics, p 914527. <https://doi.org/10.1117/12.2055320>
 22. Roll J, Thompson K (2012) Freeform optics: evolution? No, revolution! | SPIE Homepage: SPIE. <http://spie.org/newsroom/4309-freeform-optics-evolution-no-revolution?SSO=1>. Accessed 15 Nov 2018
 23. Dimmler M, Barriga P, Cayrel M, Derie F, Foerster A, Gonte F, Gonzalez JC, Jochum L, Kornweibel N, Leveque S, Lucuix C, Pettazzi L (2018) Getting ready for serial production of the segmented 39-meter ELT primary: status, challenges and strategies. In: *Ground-based and airborne telescopes VII*. Presented at the ground-based and airborne telescopes VII, international society for optics and photonics, p 1070043. <https://doi.org/10.1117/12.2312073>
 24. Crampton D, Ellerbroek B. (2005) Design and development of TMT. International Astronomical Union. In: *Proceedings of the International Astronomical Union; Cambridge*, vol 1, pp 410–419
 25. Seo B-J, Nissly C, Colavita M, Troy M, Roberts S, Rogers J (2018) Optical performance prediction of the Thirty Meter Telescope after initial alignment using optical modeling. In: *Modeling, systems engineering, and project management for astronomy VIII*. Presented at the modeling, systems engineering, and project management for astronomy VIII, international society for optics and photonics, p 107050T. <https://doi.org/10.1117/12.2314351>
 26. Stepp L (2012) Thirty Meter Telescope project update. In: *Ground-based and airborne telescopes IV*. Presented at the ground-based and airborne telescopes IV, international society for optics and photonics, p 84441G. <https://doi.org/10.1117/12.928006>
 27. Nella J, Atcheson PD, Atkinson CB, Au D, Bronowicki AJ, Bujanda E, Cohen A, Davies D, Lightsey PA, Lynch R, Lundquist R, Menzel MT, Mohan M, Pohner J, Reynolds P, Rivera H, Texter SC, Shuckstes DV, Simmons DDF, Smith RC, Sullivan PC, Waldie DD, Woods R (2004) James Webb Space Telescope (JWST) observatory architecture and performance. In: *Optical, infrared, and millimeter space telescopes*. Presented at the optical, infrared, and millimeter space telescopes, international society for optics and photonics, pp 576–588. <https://doi.org/10.1117/12.548928>
 28. Hubbard R (2013) M1 microroughness and dust contamination (no. 0013, rev. C), advanced technology solar telescope technical note
 29. Blalock T, Medicus K, Nelson JD (2015) Fabrication of freeform optics. In: *Optical manufacturing and testing XI*. Presented at the optical manufacturing and testing XI, international society for optics and photonics, p 95750H. <https://doi.org/10.1117/12.2188523>
 30. Fess E, Bechtold M, Wolfs F, Bechtold R (2013) Developments in precision optical grinding technology. In: *Optifab 2013*. Presented at the Optifab 2013, international society for optics and photonics, p 88840L. <https://doi.org/10.1117/12.2029334>
 31. Walker DD, Brooks D, King A, Freeman R, Morton R, McCavana G, Kim S-W (2003) The ‘precessions’ tooling for polishing and figuring flat, spherical and aspheric surfaces. *Opt Express* OE 11:958–964. <https://doi.org/10.1364/OE.11.000958>
 32. Gurganus D, Owen JD, Dutterer BS, Novak S, Symmons A, Davies MA (2018) Precision glass molding of freeform optics. In: *Optical manufacturing and testing XII*. Presented at the optical manufacturing and testing XII, international society for optics and photonics, p 107420Q. <https://doi.org/10.1117/12.2320574>
 33. Risse S, Scheiding S, Beier M, Gebhardt A, Damm C, Peschel T (2014) Ultra-precise manufacturing of aspherical and freeform

- mirrors for high resolution telescopes. In: Advances in optical and mechanical technologies for telescopes and instrumentation. Presented at the advances in optical and mechanical technologies for telescopes and instrumentation, international society for optics and photonics, p 91510M. <https://doi.org/10.1117/12.2056496>
34. Fang F, Xu F (2018) Recent advances in micro/nano-cutting: effect of tool edge and material properties. *Nanomanufacturing Metrol* 1:4–31. <https://doi.org/10.1007/s41871-018-0005-z>
 35. Beier M, Scheiding S, Gebhardt A, Loose R, Risse S, Eberhardt R, Tünnermann A (2013) Fabrication of high precision metallic free-form mirrors with magnetorheological finishing (MRF). In: Optifab 2013. Presented at the Optifab 2013, international society for optics and photonics, p 88840S. <https://doi.org/10.1117/12.2035986>
 36. Martin HM, Allen RG, Burge JH, Davis JM, Davison WB, Johns M, Kim DW, Kingsley JS, Law K, Lutz RD, Strittmatter PA, Su P, Tuell MT, West SC, Zhou P (2014) Production of primary mirror segments for the Giant Magellan Telescope. In: Advances in optical and mechanical technologies for telescopes and instrumentation. Presented at the advances in optical and mechanical technologies for telescopes and instrumentation, international society for optics and photonics, p 91510J. <https://doi.org/10.1117/12.2057012>
 37. Martin HM, Allen RG, Burge JH, Kim DW, Kingsley JS, Law K, Lutz RD, Strittmatter PA, Su P, Tuell MT, West SC, Zhou P (2012) Production of 8.4 m segments for the Giant Magellan Telescope. In: Modern technologies in space- and ground-based telescopes and instrumentation II. Presented at the modern technologies in space- and ground-based telescopes and instrumentation II, international society for optics and photonics, p 84502D. <https://doi.org/10.1117/12.926347>
 38. West SC, Angel R, Cuerden B, Davison W, Hagen J, Martin HM, Kim DW, Sisk B (2014) Development and results for stressed-lap polishing of large telescope mirrors I. In: Classical optics 2014 (2014), paper OTh2B.4. Presented at the optical fabrication and testing, optical society of america, p OTh2B.4. <https://doi.org/10.1364/OFT.2014.OTh2B.4>
 39. Kim DW, Martin HM, Burge JH (2011) Calibration and optimization of computer-controlled optical surfacing for large optics. In: Optical manufacturing and testing IX. Presented at the optical manufacturing and testing IX, international society for optics and photonics, p 812615. <https://doi.org/10.1117/12.893878>
 40. Cole G (2017) Optical fabrication and metrology for the thirty meter telescope primary mirror segments. In: Optical design and fabrication 2017 (Freeform, IODC, OFT) (2017), paper OW1B.4. Presented at the optical fabrication and testing, optical society of America, p OW1B.4. <https://doi.org/10.1364/OFT.2017.OW1B.4>
 41. Geyl R, Bardon D, Bourgois R, Ferachoglou N, Harel E, Couteret C (2018) First steps in ELT optics polishing. In: Fifth European seminar on precision optics manufacturing. Presented at the fifth European seminar on precision optics manufacturing, international society for optics and photonics, p 1082904. <https://doi.org/10.1117/12.2317604>
 42. Gray C, Baker I, Davies G, Evans R, Field N, Fox-Leonard T, Messelink W, Mitchell J, Rees P, Waive S, Walker DD, Yu G (2013) Fast manufacturing of E-ELT mirror segments using CNC polishing. In: Optical manufacturing and testing X. Presented at the optical manufacturing and testing X, international society for optics and photonics, p 88380K. <https://doi.org/10.1117/12.2023475>
 43. Yu G, Walker DD, Li H (2012) Research on fabrication of mirror segments for E-ELT. In: 6th international symposium on advanced optical manufacturing and testing technologies: advanced optical manufacturing technologies. Presented at the 6th international symposium on advanced optical manufacturing and testing technologies: advanced optical manufacturing technologies, international society for optics and photonics, p 841602. <https://doi.org/10.1117/12.2009290>
 44. Acosta D, Albajez JA, Yagüe-Fabra JA, Velázquez J (2018) Verification of machine tools using multilateration and a geometrical approach. *Nanomanufacturing Metrol* 1:39–44. <https://doi.org/10.1007/s41871-018-0006-y>
 45. Gallagher B, Bergeland M, Brown B, Chaney D, Copp T, Lewis J, Shogrin B, Smith K, Sokol J, Hadaway J, Glatzel H, Johnson P, Lee A, Patriarca D, Stevenson I, Cluney J, Parsonage T, Calvert J, Rodgers B, McKay A, Texter S, Cohen L, Feinberg L (2011) JWST mirror production status. In: UV/Optical/IR space telescopes and instruments: innovative technologies and concepts V. Presented at the UV/Optical/IR space telescopes and instruments: innovative technologies and concepts V, international society for optics and photonics, p 814607. <https://doi.org/10.1117/12.892326>
 46. Trumper I, Jannuzi BT, Kim DW (2018) Emerging technology for astronomical optics metrology. *Opt Lasers Eng Opt Tools Metrol Imaging Diagn* 104:22–31. <https://doi.org/10.1016/j.optlaseng.2017.09.009>
 47. Rees PCT, Gray C (2015) Metrology requirements for the serial production of ELT primary mirror segments. In: Optical manufacturing and testing XI. Presented at the optical manufacturing and testing XI, international society for optics and photonics, p 957508. <https://doi.org/10.1117/12.2189783>
 48. Bos A, Henselmans R, Rosielle PCJN, Steinbuch M (2015) Nanometre-accurate form measurement machine for E-ELT M1 segments. *Precis Eng* 40:14–25. <https://doi.org/10.1016/j.precisioneng.2014.09.008>
 49. Mueller U (2016) Production metrology design and calibration for TMT primary mirror fabrication used at multiple manufacturing sites. In: Ground-based and airborne telescopes VI. Presented at the ground-based and airborne telescopes VI, international society for optics and photonics, p 99060Z. <https://doi.org/10.1117/12.2232036>
 50. Anderson DS, Burge JH (1995) Swing-arm profilometry of aspherics. In: Optical manufacturing and testing. Presented at the optical manufacturing and testing, international society for optics and photonics, pp 169–180. <https://doi.org/10.1117/12.218421>
 51. Callender MJ, Efstathiou A, King CW, Walker DD, Gee AE, Lewis AJ, Oldfield S, Steel RM (2006) A swing arm profilometer for large telescope mirror element metrology. In: Optomechanical technologies for astronomy. Presented at the optomechanical technologies for astronomy, international society for optics and photonics, p 62732R. <https://doi.org/10.1117/12.671304>
 52. Su P, Wang Y, Oh CJ, Parks RE, Burge JH (2011) Swing arm optical CMM: self calibration with dual probe shear test. In: Optical manufacturing and testing IX. Presented at the optical manufacturing and testing IX, international society for optics and photonics, p 81260W. <https://doi.org/10.1117/12.894203>
 53. Zhang P, Li J, Yu G, Walker DD (2016) Development of swinging part profilometer for optics. In: Optics and measurement international conference 2016. Presented at the optics and measurement international conference 2016, international society for optics and photonics, p 101510B. <https://doi.org/10.1117/12.2256295>
 54. Zobrist TL, Burge JH, Martin HM (2009) Laser tracker surface measurements of the 8.4 m GMT primary mirror segment. In: Optical manufacturing and testing VIII. Presented at the optical manufacturing and testing VIII, international society for optics and photonics, p 742613. <https://doi.org/10.1117/12.826706>
 55. Jang Y-S, Kim S-W (2018) Distance measurements using mode-locked lasers: a review. *Nanomanufacturing Metrol* 1:131–147. <https://doi.org/10.1007/s41871-018-0017-8>
 56. Knauer MC, Kaminski J, Hausler G (2004) Phase measuring deflectometry: a new approach to measure specular free-form surfaces. 366–376. <https://doi.org/10.1117/12.545704>

57. Huang R, Su P, Horne T, Zappellini GB, Burge JH (2013) Measurement of a large deformable aspherical mirror using SCOTS (Software Configurable Optical Test System). In: Optical manufacturing and testing X. Presented at the optical manufacturing and testing X, international society for optics and photonics, p 883807. <https://doi.org/10.1117/12.2024336>
58. Su T, Park WH, Parks RE, Su P, Burge JH (2011) Scanning long-wave optical test system: a new ground optical surface slope test system. In: Optical manufacturing and testing IX. Presented at the optical manufacturing and testing IX, international society for optics and photonics, p 81260E. <https://doi.org/10.1117/12.892666>
59. Oh CJ, Lowman AE, Smith GA, Su P, Huang R, Su T, Kim D, Zhao C, Zhou P, Burge JH (2016) Fabrication and testing of 4.2 m off-axis aspheric primary mirror of Daniel K. Inouye Solar Telescope. Advances in optical and mechanical technologies for telescopes and instrumentation II. <https://doi.org/10.1117/12.2229324>
60. Yoo H, Smith GA, Oh CJ, Lowman AE, Dubin M (2018) Improvements in the scanning long-wave optical test system. In: Optical manufacturing and testing XII. Presented at the optical manufacturing and testing XII, international society for optics and photonics, p 1074216. <https://doi.org/10.1117/12.2321265>
61. Allen R, Su P, Burge JH, Cuerden B, Martin HM (2010) Scanning pentaprism test for the GMT 8.4-m off-axis segments. In: Modern technologies in space- and ground-based telescopes and instrumentation. Presented at the modern technologies in space- and ground-based telescopes and instrumentation, international society for optics and photonics, p 773911. <https://doi.org/10.1117/12.857901>
62. Schulz M, Ehret G, Kfen P (2013) High accuracy flatness metrology within the European metrology research program. Nuclear instruments and methods in physics research section A: accelerators, spectrometers, detectors and associated equipment. In: The 4th international workshop on metrology for x-ray optics, mirror design, and fabrication, vol 710, pp 37–41. <https://doi.org/10.1016/j.nima.2012.10.112>
63. Huang R (n.d.) High precision optical surface metrology using deflectometry. The University of Arizona. <http://hdl.handle.net/10150/581252>
64. Kim DW, Burge JH, Davis JM, Martin HM, Tuell MT, Graves LR, West SC (2016) New and improved technology for manufacture of GMT primary mirror segments. In: Advances in optical and mechanical technologies for telescopes and instrumentation II. Presented at the advances in optical and mechanical technologies for telescopes and instrumentation II, international society for optics and photonics, p 99120P. <https://doi.org/10.1117/12.2231911>
65. Huang R, Su P, Burge JH, Huang L, Idir M (2015) High-accuracy aspheric x-ray mirror metrology using Software Configurable Optical Test System/deflectometry. OE, OPEGAR 54:084103. <https://doi.org/10.1117/1.OE.54.8.084103>
66. Maldonado AV, Su P, Burge JH (2014) Development of a portable deflectometry system for high spatial resolution surface measurements. Appl Opt, AO 53:4023–4032. <https://doi.org/10.1364/AO.53.004023>
67. Lowman AE, Smith GA, Harrison L, West SC, Oh CJ (2018) Measurement of large on-axis and off-axis mirrors using software configurable optical test system (SCOTS). In: Advances in optical and mechanical technologies for telescopes and instrumentation III. Presented at the advances in optical and mechanical technologies for telescopes and instrumentation III, international society for optics and photonics, p 107061E. <https://doi.org/10.1117/12.2313855>
68. Chen S, Xue S, Dai Y, Li S (2017) Subaperture stitching test of convex aspheres by using the reconfigurable optical null. Opt Laser Technol 91:175–184. <https://doi.org/10.1016/j.optla.stec.2016.12.026>
69. Scheiding S, Beier M, Zeitner U-D, Risse S, Gebhardt A (2013) Freeform mirror fabrication and metrology using a high performance test CGH and advanced alignment features. In: Advanced fabrication technologies for micro/nano optics and photonics VI. Presented at the advanced fabrication technologies for micro/nano optics and photonics VI, international society for optics and photonics, p 86130J. <https://doi.org/10.1117/12.2001690>
70. Zhou P, Martin H, Zhao C, Burge JH (2012) Mapping distortion correction for GMT interferometric test. In: Imaging and applied optics technical papers (2012), paper OW3D.2. Presented at the optical fabrication and testing, optical society of America, p OW3D.2. <https://doi.org/10.1364/OFT.2012.OW3D.2>
71. Hadaway JB, Wells C, Olczak G, Waldman M, Whitman T, Cosentino J, Connolly M, Chaney D, Telfer R (2016) Performance of the primary mirror center-of-curvature optical metrology system during cryogenic testing of the JWST Pathfinder telescope. In: Space telescopes and instrumentation 2016: optical, infrared, and millimeter wave. Presented at the space telescopes and instrumentation 2016: optical, infrared, and millimeter wave, international society for optics and photonics, p 99044E. <https://doi.org/10.1117/12.2234741>
72. Gray P, Ciattaglia E, Dupuy C, Gago F, Guisard S, Marrero J, Ridings R, Wright A (2016) E-ELT assembly, integration, and technical commissioning plans. In: Ground-based and airborne telescopes VI. Presented at the ground-based and airborne telescopes VI, international society for optics and photonics, p 99060X. <https://doi.org/10.1117/12.2230965>
73. Zimmerman DC (2010) Feasibility studies for the alignment of the Thirty Meter Telescope. Appl Opt, AO 49:3485–3498. <https://doi.org/10.1364/AO.49.003485>
74. Troy M, Chanan G, Michaels S, Dekens F, Hein R, Herzig S, Karban R, Nissly C, Roberts J, Rud M, Seo B-J (2016) The alignment and phasing system for the Thirty Meter Telescope: risk mitigation and status update. In: Ground-based and airborne telescopes VI. Presented at the ground-based and airborne telescopes VI, international society for optics and photonics, p 99066A. <https://doi.org/10.1117/12.2231913>
75. van Dam MA, McLeod BA, Bouchez AH (2016) Dispersed fringe sensor for the Giant Magellan Telescope. Appl Opt, AO 55:539–547. <https://doi.org/10.1364/AO.55.000539>
76. Kopon D, McLeod B, Bouchez A, Catropa D, van Dam MA, Frostig D, Kansky J, McCracken K, Podgorski W, McMuldrough S, D'Arco J, Close L, Males JR, Morzinski K (2018) Preliminary on-sky results of the next generation GMT phasing sensor prototype. In: Adaptive optics systems VI. Presented at the adaptive optics systems VI, international society for optics and photonics, p 107030X. <https://doi.org/10.1117/12.2314381>
77. Bouchez AH, McLeod BA, Acton DS, Kanneganti S, Kibblewhite EJ, Shectman SA, van Dam MA (2012) The Giant Magellan Telescope phasing system. In: Adaptive optics systems III. Presented at the adaptive optics systems III, international society for optics and photonics, p 84473S. <https://doi.org/10.1117/12.927163>
78. Xin B, Claver C, Liang M, Chandrasekharan S, Angeli G, Shipsey I (2015) Curvature wavefront sensing for the large synoptic survey telescope. Appl Opt, AO 54:9045–9054. <https://doi.org/10.1364/AO.54.009045>
79. DeVries J, Neill DR, Barr J, Lorenzi SD, Marchiori G (2016) The LSST dome final design. In: Ground-based and airborne telescopes VI. Presented at the ground-based and airborne telescopes VI, international society for optics and photonics, p 99060N. <https://doi.org/10.1117/12.2233320>
80. Murga G, Marshall H, Ariño J, Lorentz T (2012) ATST enclosure final design and construction plans. In: Ground-based and

- airborne telescopes IV. Presented at the ground-based and airborne telescopes IV, international society for optics and photonics, p 844408. <https://doi.org/10.1117/12.925987>
81. Teran J, Sheehan M, Neff DH, Korde N, Manuel E, Ortega A (2014) GMT enclosure structure and mechanism design. In: Ground-based and airborne telescopes V. Presented at the ground-based and airborne telescopes V, international society for optics and photonics, p 91454L. <https://doi.org/10.1117/12.2055189>
 82. Bilbao A, Murga G, Gómez C, Llarena J (2014) Approach to the E-ELT dome and main structure challenges. In: Ground-based and airborne telescopes V. Presented at the ground-based and airborne telescopes V, international society for optics and photonics, p 91452J. <https://doi.org/10.1117/12.2054866>
 83. Stanghellini S, Martinez P, Kraus M (2018) Procurement of the dome and the telescope structure of the ESO ELT: status report. In: Ground-based and airborne telescopes VII. Presented at the ground-based and airborne telescopes VII, international society for optics and photonics, p 1070009. <https://doi.org/10.1117/12.2313510>
 84. Thomas-Osip JE, McCarthy P, Prieto G, Phillips MM, Johns M (2010) Giant Magellan Telescope site testing: summary. In: Ground-based and airborne telescopes III. Presented at the ground-based and airborne telescopes III, international society for optics and photonics, p 77331L. <https://doi.org/10.1117/12.856934>
 85. Teran J, Burgett WS, Grigel E, Bigelow BC, Donoso E, Figueroa F (2016) GMT site, enclosure, and facilities design and development overview and update. In: Ground-based and airborne telescopes VI. Presented at the ground-based and airborne telescopes VI, international society for optics and photonics, p 990610. <https://doi.org/10.1117/12.2232573>
 86. Teran J, Sanders G, Falcon G, Adriaanse D, Gillett P, Dumas C (2018) Alternate site selection and development for the Thirty Meter Telescope at Observatorio del Roque de los Muchachos, La Palma, Spain. In: Ground-based and airborne telescopes VII. Presented at the ground-based and airborne telescopes VII, international society for optics and photonics, p 1070053. <https://doi.org/10.1117/12.2313646>
 87. Warner M, Rimmele TR, Pillet VM, Casini R, Berukoff S, Craig SC, Ferayorni A, Goodrich BD, Hubbard RP, Harrington D, Jeffers P, Johansson EM, Kneale R, Kuhn J, Liang C, Lin H, Marshall H, Mathioudakis M, McBride WR, McMullin J, McVeigh W, Sekulic P, Schmidt W, Shimko S, Sueoka S, Summers R, Tritschler A, Williams TR, Wöger F (2018) Construction update of the Daniel K. Inouye Solar Telescope project. In: Ground-based and airborne telescopes VII. Presented at the ground-based and airborne telescopes VII, international society for optics and photonics, p 107000V. <https://doi.org/10.1117/12.2314212>



Logan R. Graves is a Ph.D. candidate in the College of Optical Sciences at the University of Arizona. His main research area covers precision optical metrology, focusing on deflectometry hardware and software development for improved freeform measurement capabilities. He also has a background in biomedical engineering, with research topics including early

cancer detection utilizing autofluorescence and non-linear rod-cone interactions at the retinal level.



Greg A. Smith conducts research in large optics manufacturing and testing at the College of Optical Sciences, University of Arizona. He received his optics Ph.D. in 2006 and specializes in the areas of polarization optics and software algorithms for optical metrology. His experience ranges from development of computer controlled polishing systems for a 4m off-axis parabola to metrology tools which can measure optical grit surfaces with 40-micron grit surface finish.



Dániel Apai is an associate professor at the Steward Observatory and the Lunar and Planetary Laboratory of The University of Arizona. He is specializing in studies of extrasolar planets with the goal of identifying planetary systems capable of supporting life. He is leading major programs on the Hubble and Spitzer Space Telescopes, and also regularly uses the largest ground-based telescopes for his studies. Dr. Apai is currently serving on the Giant Magellan Telescope Science Advisory Committee

and on the Steering Committee of the NASA Nexus for Exoplanet System Science.



Dae Wook Kim is an assistant professor of optical sciences and astronomy at the University of Arizona. He has been working in the optical engineering field for more than 10 years, mainly focusing on very large astronomical optics, such as the 25 m diameter Giant Magellan Telescope primary mirrors. His main research area covers precision freeform optics fabrication and various metrology topics, such as interferometric test systems using computer generated holograms, direct curvature measurements,

and dynamic deflectometry systems. He is currently a chair of the Optical Manufacturing and Testing conference (SPIE), Optical Fabrication and Testing conference (OSA), and Astronomical Optics: Design, Manufacture, and Test of Space and Ground Systems conference (SPIE). He is a senior member of OSA and SPIE and has been serving as an associate editor for the journal *Optics Express*.